Distribution Agreement

In presenting this thesis as a partial fulfillment of the requirements for a degree from Emory University, I hereby grant to Emory University and its agents the non-exclusive license to archive, make accessible, and display my thesis in whole or in part in all forms of media, now or hereafter known, including display on the world wide web. I understand that I may select some access restrictions as part of the online submission of this thesis. I retain all ownership rights to the copyright of the thesis. I also retain the right to use in future works (such as articles or books) all or part of this thesis.

Signature:

_____ _____

Victoria S. Jiang April 9, 2013

Synthesis and Characterization of Organic and Inorganic Compounds with Biological and Material Applications

By

Victoria S. Jiang

Advisor: Frank E. McDonald, PhD

Department of Chemistry

In collaboration with:

W. Charles O'Neill, MD

_____

Frank E. McDonald, Advisor

_____

W. Charles O'Neill, Advisor

_____

Jose D. Soria, Committee Member

_____

April 9, 2013

Synthesis and Characterization of Organic and Inorganic Compounds with Biological and Material Applications

By

Victoria Jiang

Advisor: Frank E. McDonald, PhD

An abstract of a thesis submitted to the Faculty of Emory College of Arts and Sciences of Emory University in partial fulfillment of the requirements of the degree of Bachelor of Sciences with Honors

Department of Chemistry

2013

Abstract

Synthesis and Characterization of Organic and Inorganic Compounds with Biological and Material Applications

The synthesis of an iodonium-bridge activated cyclization model system is reported. A six-membered heterocyclic ether was synthesized through a seven-step linear synthesis using iodine as the activator. The cyclic ether product serves as a model system for generation of the *trans-syn-trans* stereochemistry displayed within the brevetoxin family. The results suggest that the *trans*-alkene diol generates a cyclic ether with *trans-anti-trans* stereochemistry.

A three-step synthetic route to septanose glycal from D-(-)-ribose is also reported. These seven-membered sugar rings can be polymerized to generate biopolymers capable of novel and predictable biological activity. This synthesis includes a one-carbon homologation of acetonide-protected ribofuranose using the Bestmann-Ohira modification of the Seyferth-Gilbert homologation. The subsequent alkynyl diol will be converted to a septanose carbohydrate using a $W(CO)_6$-catalyzed cyclization reaction.

Lastly, the progress towards the synthesis and characterization of monothiopyrophosphate is reported. This pyrophosphate derivative is a promising therapeutic candidate for inhibition of vascular calcification characteristic of patients with increasing age, renal disease and diabetes.

Synthesis and Characterization of Organic and Inorganic Compounds with Biological and Material Applications

By

Victoria S. Jiang

Advisor: Frank E. McDonald

A thesis submitted to the Faculty of Emory College of Arts and Sciences of Emory University in partial fulfillment of the requirements of the degree of Bachelor of Sciences with Honors

Department of Chemistry

2013

Acknowledgements

First and foremost, I would like to thank the Emory University Department of Chemistry, Emory School of Medicine Department of Nephrology, the Emory SURE program, the American Heart Association (11GRNT7660009), the Emory SIRE program, the Center for Science Education and the Office of Undergraduate Education for supporting this research. Three wonderful women, Dr. Cathy Quinones, Dr. Pat Marsteller, and Dr. Leah Roesch have provided numerous accounts of support and guidance that have invaluably shaped my respect and adoration of science. Also, I would like to thank the NSF and NIH for shared instrumentation available to Emory.

I would like to thank several peers and colleagues that have helped me throughout my research experience. Since my first day in lab, Kristen Stoltz took me under her wing and was instrumental in the development of my lab techniques. Dr. Kento Ishida aided in synthetic methods and structure elucidation for the iodocyclization project while Dr. Shaoxiong Wu aided in ^{31}P NMR data acquisition and analysis. I would like to thank Jack Trieu, Jessica Hurtak, and members of the McDonald lab for continual motivation through the daily trails of research.

Lastly, I would like to acknowledge the enormous role that my academic and research advisors played in my personal and professional development throughout college. Dr. Jose Soria gave a naïve freshman girl a taste of organic chemistry and the ability to laugh at her own quarks. Dr. Jaap de Roode taught me the foundations of evolution, a reminder of the need to continually improve and adapt daily. Dr. Charles O'Neill showed me the intricacies of medicinal chemistry and sharpened my ability to critically interpret data. Through it all, I would like to thank Dr. Frank McDonald for continually believing in me and showing me the beauty of organic synthesis. Through thick and thin, he taught me valuable lessons both in and out of lab. Without the guidance of my advisors, I would be nowhere.

Table of Contents

I. Stereoselectivity of hydroxyalkene cyclizations: Model systems for the synthesis of marine polycyclization products

1. Introduction

Karenia brevis and *Gambierdiscus toxicus* are two marine dinoflagellates responsible for synthesizing these stereochemically unique toxins that have resulted in mass fish killings during organismal blooming in both the Atlantic and Pacific oceans respectively[1]. These organisms are known for causing the red tide, a wave of toxins resulting in not only killing fish and manatees but also humans who ingest affected fish. These algal blooms have been documented back to the Spanish Inquisition, with each bloom threatening the fragile ecosystem[1]. These organisms are most noted for the synthesis of brevetoxin A (Figure 1) and B (Figure 2). Brevetoxins A and B are members of a larger family of marine toxins that consist of complex trans-fused polycyclic alternating six, seven, eight and nine membered ether rings. These molecules have a distinctive *trans-syn-trans* stereochemistry, resulting in a rigid ladder structure that can possess over twenty chiral centers. Within the same class of toxins, *G. toxicus* is responsible for synthesizing maitotoxin (Figure 3), the largest naturally occurring molecule aside from biopolymers such as DNA, RNA and proteins. Not only is it the largest, but it is also the most potent toxin known with a lethal dose of 0.17μg/kg in mice[1]. Besides brevetoxins A and B, *K. brevis* also produce brevenal (Figure 4), a nontoxic competitive inhibitor of brevetoxin receptor site binding. Not only does brevenal act to inhibit brevetoxin A and B binding, it also serves as tracheal mucus accelerator and an innocuous antagonist at the brevetoxin binding site.[1]

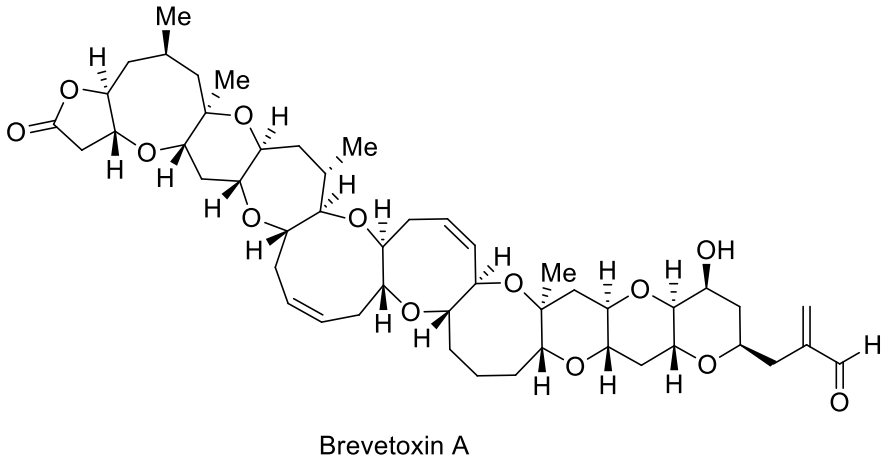

Figure 4. Molecular Structure of Brevetoxin A[1]

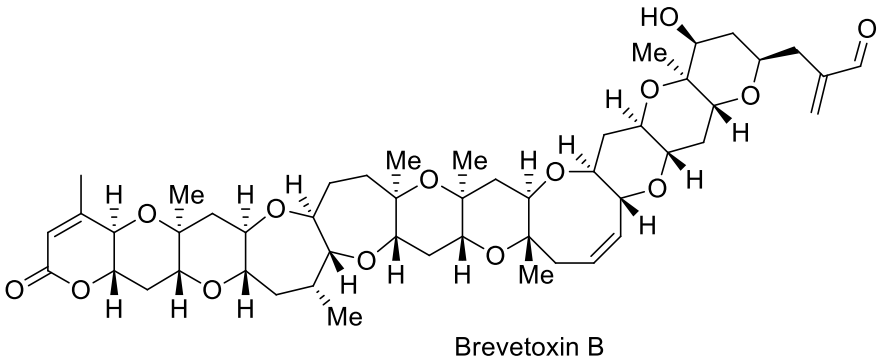

Figure 5. Molecular structure of Brevetoxin B[1]

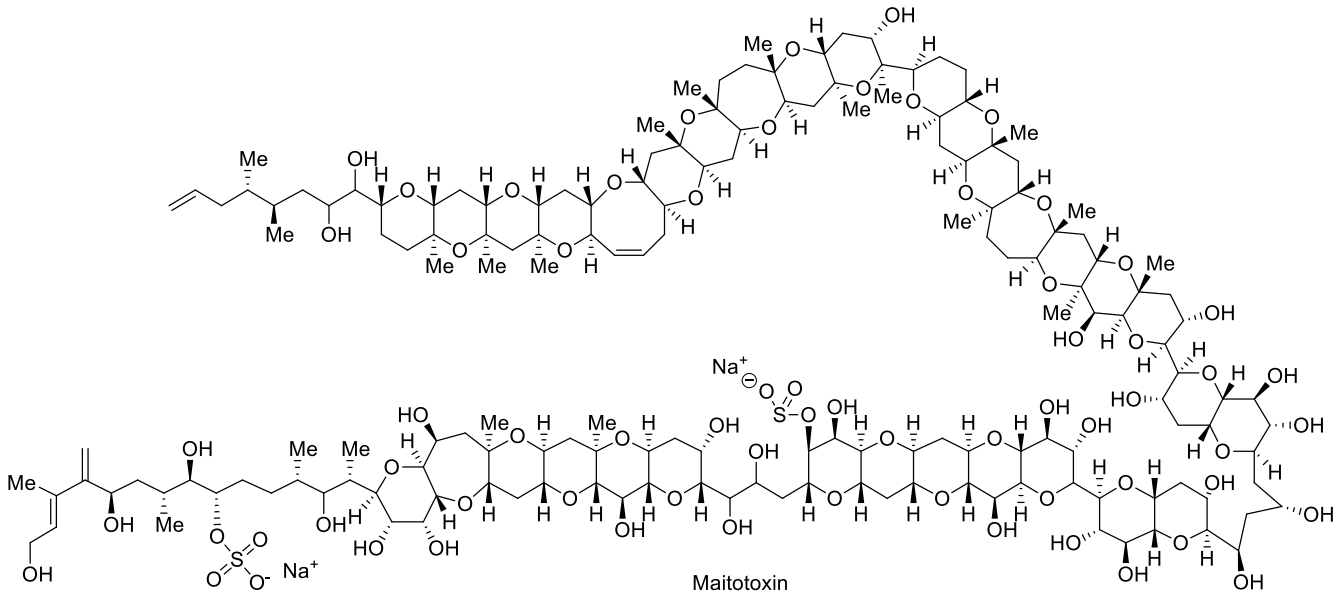

Figure 6. Molecular structure of Maitotoxin.[1]

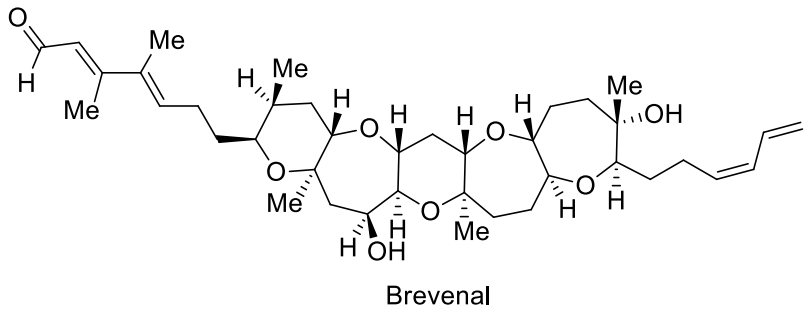

Figure 7. Molecular structure of brevenal[1]

The brevetoxins and all natural known derivatives share a number of key characteristics shown Figure 4. The "rigid" region, rings H-K, is involved in inactivating membrane potential-gated ion channels upon ingestion or inhalation. All bioactive toxins and derivatives of the brevetoxin family possess this ring structure. The A-Ring or "head" region of the molecule usually consists of a five or six member ring with lactone functionality. This region moderates mean opening time and inactivation responses when bound to the ligand-gated ion channels. The "spacer" region, rings B-E, separates the head and rigid regions of the molecule and have limited flexibility. The "tail" region is a hydrocarbon side chain that varies among the toxins.[4]

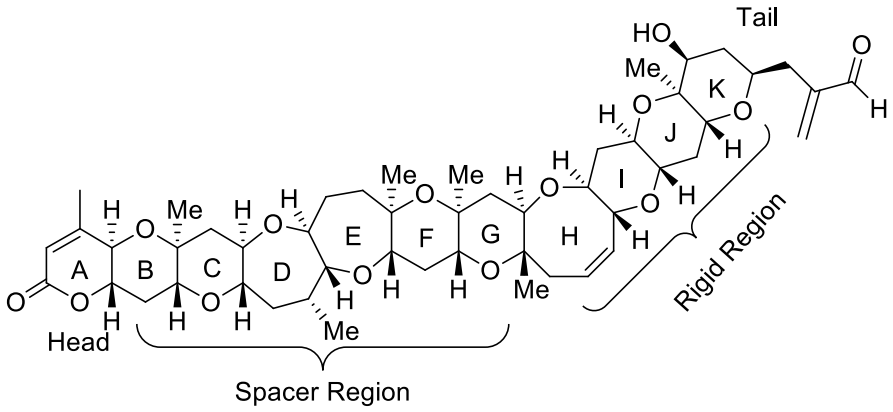

Figure 8. Characteristic regions of the brevetoxin family.[4]

When bound to receptor site 5 on the voltage-sensitive sodium channels (VSSCs), these lipid-soluble toxins cause complete depolarization of the channels at resting state and inhibition of inactivation. Normally, the channel opens in response to membrane depolarization and inactivate for repolarization.

Allosteric realignment upon ligand-binding causes the channel to change configuration from "closed" to "open"[4]. Binding causes four distinct responses from the channels: 1) activation potential is shifted towards more negative potentials, favoring channel opening at normal resting potential; 2) longer average opening time; 3) an increase of sodium ion influx; and 4) an inhibition of inactivation which results in channel closing[4]. Prolonged channel opening can disrupt the neurological signals between the ion channels to the nervous system[1].

When the algae bloom, the organisms use granules as airborne vehicles to launch the toxin into the surrounding environment. If inhaled, brevetoxins can cause non-productive coughs and bronchoconstriction, decreasing the tracheal mucus velocity (TMV)[1]. If ingested either directly or indirectly through affected prey, the toxins can cause neurotoxic shellfish poisoning (NSP)[1]. Known symptoms of NSP include gastroenteritis, tunnel vision and dizziness. Aside from NSP, clinical studies have shown that brevetoxin exposure, particularly on beaches during algae bloom along the Gulf of Mexico, can increase the likelihood to experience broncho-irritation and asthmatic behavior[3].Synthesis of brevetoxins can be used in investigating bioactivity and further developing our understanding of the toxin's pathology[1]. The structure and character of the brevetoxin family can give vital stereochemical and medicinal information pertaining to the biological effects of these natural products and related analogs. The *trans-syn-trans* stereochemistry gives this family of molecules a distinctive rigid ladder structure specific to the VSSC binding sites and is responsible for the biological pathologies. If these macromolecules did not possess this specific stereochemistry, the molecules would wrap around in cylindrical fashion to a cup-like structure instead of the rigid ladder-like structure.

The first structure elucidation of Brevetoxin B was done in 1981[8,9]. Due to the complexity of the molecule, a number of total syntheses have been reported where novel cyclizations methods of the cyclic ether motifs. Nicoloau et al[5] reported a convergent 123 step total synthesis of Brevetoxin B

where the last step entailed coupling the spacer and rigid region components and using Ph_3SnH to induce a radical cyclization forming the final connecting H-ring (Scheme 1).

In order to obtain the spacer and rigid coupling components, Nicoleau utilized a number of Lewis acid catalyzed epoxide openings[6] and hydroxyl dithioketal cyclization[7] to cyclize each individual ring as shown in Scheme 1.

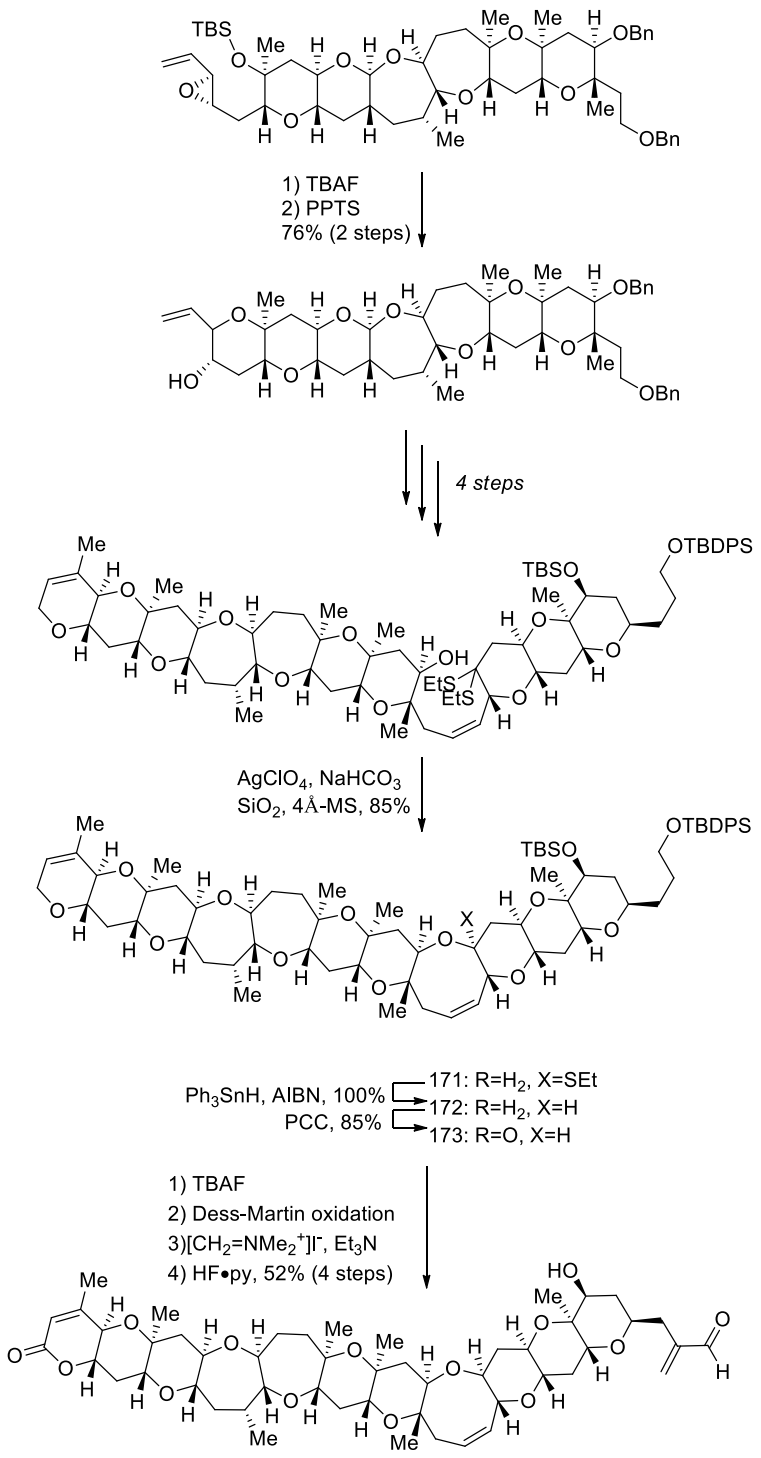

Scheme 1. Nicoloau's synthesis of Brevetoxin B.[5,6]

Nakata et al.[10] used a similar convergent strategy, reporting an alternative synthesis of Nicoleau's intermediates but coupling them together in the same fashion. Most notably, Nakata's total synthesis incorporated a SmI_2-induced cyclization[12] forming two ether rings along the spacer region in

a concerted fashion possessing the correct *trans-syn-trans* stereochemistry. In addition, they utilized ring-closing olefin metathesis[11] and SmI_2-induced intramolecular Reformatsky-type reaction[13]. Most notable reactions for forming polycyclic ether rings are shown in Scheme 2.

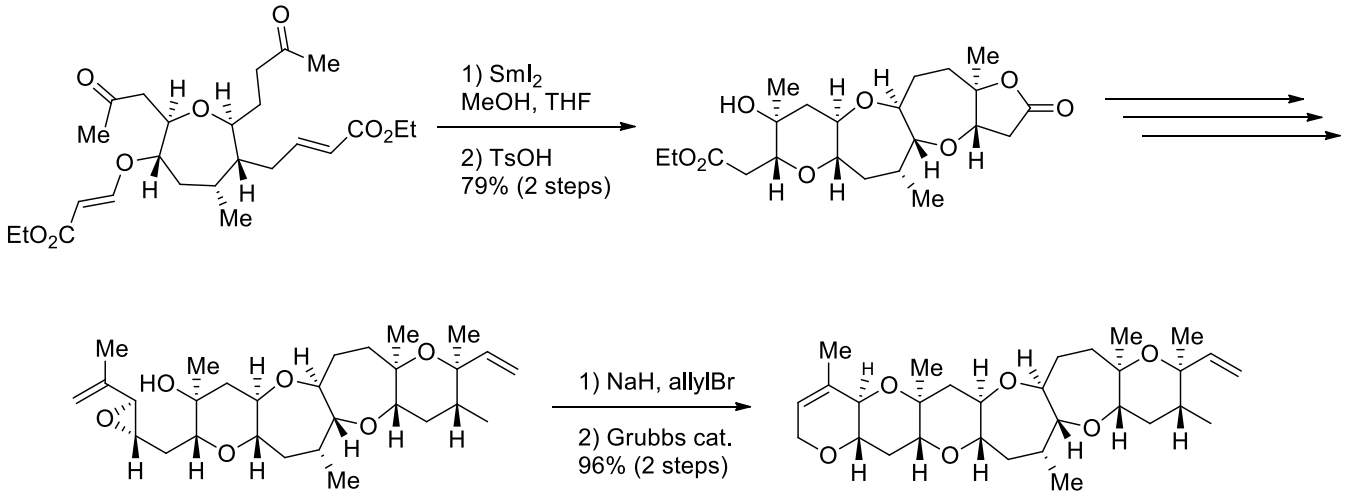

Scheme 2. Key reactions developed by Nakata et al for the convergent total synthesis of Brevetoxin B[11,12,13]

The biomimetic pathway was thought to be composed of epoxide openings through a concerted electron cascade. In previous studies, McDonald et al. explored concerted polyepoxide ring openings originally derived from terpenes as shown in Figure 6. Compound **1** was transformed into the desired polyoxepanes through the Sharpless epoxidation of the allylic alcohol[1]. The subsequent alkenes were transformed into chiral epoxides through the Shi epoxidation. The stereochemistry of these polyoxepanes was congruent with the desired electron cascade proposal through the cascade initiation by a terminal carbonate. The cyclization was carried out with $BF_3{\bullet}OEt_2$ to afford the polycyclic ether backbone as shown in Scheme 3. While the end result possessed the desired *trans-syn-trans*-stereochemistry, the backbone generated is not ultimately similar to the backbone of the desired brevetoxin family and can only be produced in low to moderate yields. This method proved to be successful in generating seven-member rings through 7-*endo* cyclizations instead of desired six member polycyclic ring formation. The study verifies the formation of *trans-syn-trans*-substituted polypyrans and polyoxepanes through disfavored 6-*endo* and 7-*endo* oxacyclizations.[1] The regioselective tandem

cyclizations are effective and can be potentially extended to a more concise total synthesis of derivatives of the brevetoxin family.

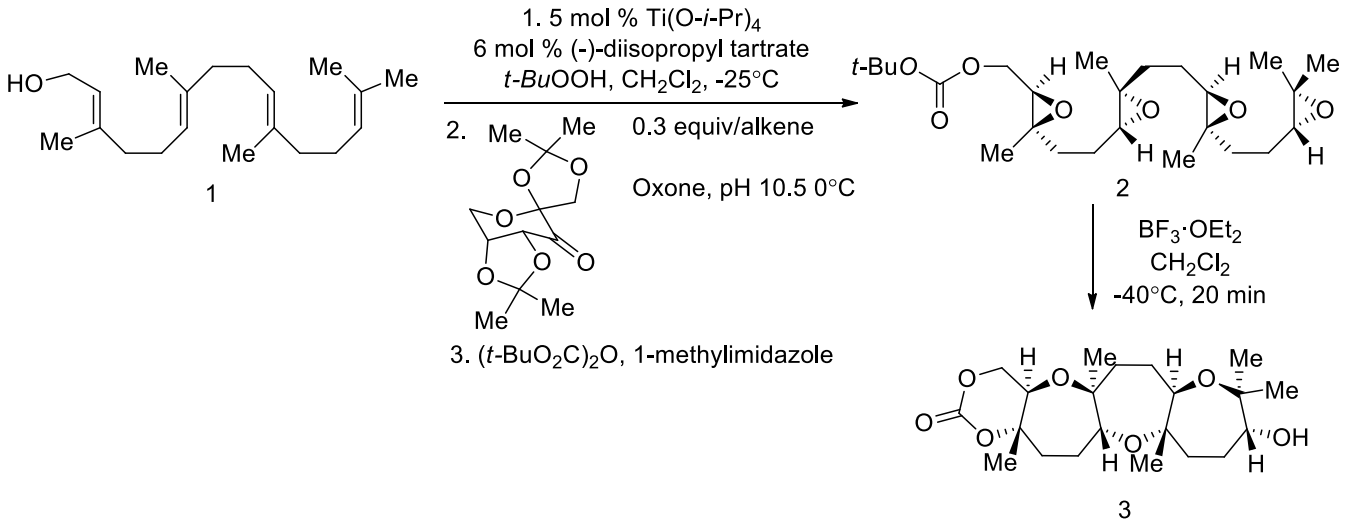

Scheme 3. McDonald's method of tandem cyclization through polyepoxidation.[1]

Another avenue to explore would be the hydroxyalkene cyclizations through the addition of iodine. Instead of pursuing the kinetically disfavorable 6-*endo* route, the iodonium-bridge activated cyclization can proceed through a 6-*exo* cyclization, which is kinetically favorable based on Baldwin's rules. Rather than using a number of protections and functional group manipulation, a 6-*exo* cyclization can lead to concerted stereoselective formation of our desired polycyclic product. The activation of the alkene using an iodoether formation would provide a sterically selective cyclization. Chamberlin et al. have explored the cyclization of iodoethers in this fashion, and while the species cyclized and produced the desired stereochemistry, there was a poor yield, thermodynamically favoring a 6,5-skeleton.[2] When run with I_2 and acetonitrile, however, the desired 6,6-isomer was able to be synthesized with 90% yield. When trying to add the hydroxyl group, however, the process favored the *trans-anti-trans* formation [2]. Some steric directors have been explored like $AgBF_4$ to maintain the stereochemistry when the hydrolysis was preformed [2].

The goal of this project is to create a model system for synthesizing trans-syn-trans polycyclic ether rings. This project will outline a universal protocol for a model substrate that is stereoselective in the ether ring formation. The trans-syn-trans cyclization will result from a hydroxyalkene cyclization where iodine activates the alkene as shown in Figure 7. Herein, we propose a synthesis towards the iodonium-activated cyclization shown in Figure 7. Commercially available compound **6** will be converted to trans-alkene **4** as the target substrate of the iodonium-activated cyclization.

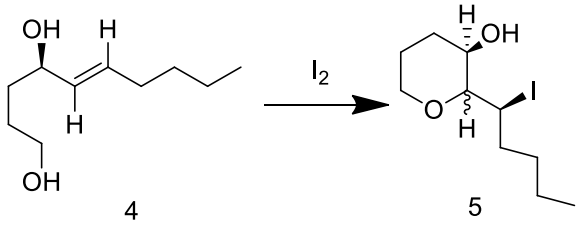

Figure 9. Proposed Iodine activated hydroxyalkene cyclization.

2. Experimental

2.1 General Experimental Procedures

All commercially available reagents were purchased from Sigma-Aldrich, Inc. All reagents were used without further purification. ^{1}H NMR studies used for structure elucidation were performed on the Varian INOVA 400 spectrometer at 400 MHz in $CDCl_3$, using the $CDCl_3$ singlet at 7.26 ppm as an internal reference. All reactions were conducted in oven-dried round bottom flasks under an inert argon atmosphere.

2.2.1 *4-((tert-butyldimethylsilyl)oxy)butanal (**7**)*: To an oven dried 250 mL round bottom flask equipped with metallic stirbar under argon, **6** (10.0 g, 48.9 mmol, 1.0 equiv), TEA (9.90 g, 97.8 mmol, 2.00 equiv), and DMSO (7.65 g, 97.8 mmol, 2.0 equiv) were taken in dry CH_2Cl_2 (70.0 mL). The reaction mixture was cooled to 0°C with an ice water bath. Sulfur trioxide pyridine complex (15.6 g, 97.8 mmol, 2.0 equiv) was added and the orange-red reaction mixture was warmed to room temperature

and stirred for two hours. The reaction mixture was quenched with deionized water (18 mL). The organic layer was extracted with CH_2Cl_2 (3x15 mL) dried over $MgSO_4$, filtered, and concentrated under vacuum on a rotary evaporator. The crude oil was purified using column chromatography with 230-400 mesh silica gel and a 95:5 mixture of hexanes:EtOAc as the eluent to afford the desired compound, **7** in a 57.5% yield (5.72 g) as a colorless oil. ^{1}H NMR (400 MHz, $CDCl_3$) δ 9.79 (t, *J* = 1.6 Hz, 1H), 3.66 (t, *J* = 6.0 Hz, 2H), 2.51 (dt, *J* = 6.8, 1.6 Hz, 2H), 1.87 (qt, *J* = 6 Hz, 2H), 0.85 (s, 9H), 0.12 (s, 6H).

2.2.2 *(R)-1-((tert-butyldimethylsilyl)oxy)dec-5-yn-4-ol (**8**)*: To an oven dried 100 mL round bottom flask equipped with metallic stirbar under argon, 1-hexyne (1.02 g, 12.37 mmol, 1.00 eq) and *n*-butyllithium (0.87 g, 13.60 mmol, 1.10 equiv) were taken in dry THF (50 mL) and cooled to 0°C in an ice water bath. The reaction mixture was stirred for 15 minutes then **7** (2.50 g, 12.37 mmol, 1.00 equiv) was added dropwise. The reaction mixture was maintained at 0°C and stirred for 2.5 hours. The reaction mixture was quenched with color coded yellow buffer solution (pH 7.0, 15 mL). The organic layer was extracted with EtOAc (3x15 mL) and washed with deionized water (3x15 mL). The organic layer was dried over $MgSO_4$, filtered, and concentrated under vacuum on a rotary evaporator to afford a colorless oil. The crude oil was purified by column chromatography with 230-400 mesh silica gel and a 95:5 mixture of hexanes:EtOAc as the eluant to afford the desired compound, **8** in a 66.2% yield (2.329 g) as a colorless oil. ^{1}H NMR (400 MHz, $CDCl_3$) δ 3.70 (m, 2H), 2.21 (dt, *J* = 6.8, 1.6 Hz, 2H), 1.78 (m, 3H), 1.45 (m, 3H), 1.26 (m, 3H), 0.91 (s, 12H), 0.09 (s, 6H).

2.2.3 *(R,E)-dec-5-ene-1,4-diol (**4**)*: To an oven dried 100 mL round bottom flask equipped with metallic stirbar under argon, **8** (2.3 g, 8.09 mmol, 1.0 equiv) was taken in dry Et_2O (45 mL) and cooled to 0°C in an ice water bath. Vitride [Red-Al® sodium bis(2-methoxyethoxy)aluminum hydride solution 65% w/w in toluene] (3.75 g, 12.04 mmol, 1.5 equiv) was added dropwise to the reaction mixture. The reaction mixture stirred at 0°C for two hours and then warmed to room temperature and stirred overnight. The reaction mixture was quenched with a saturated aqueous solution of Rochelle's salt

(potassium sodium tartrate, 20 mL). The organic layer was extracted with EtOAc (3x15 mL) and washed with brine (2x15 mL). The crude mixture was dried over $MgSO_4$, filtered, and concentrated under vacuum on a rotary evaporator to afford a colorless oil. The crude oil **9** was carried over for deprotection. To an oven dried 100 mL round bottom flask equipped with metallic stirbar under argon, the crude oil was taken in dry THF (50 mL) at room temperature. TBAF (2.04 g, 7.8 mmol, 1.5 equiv) was added dropwise to the reaction mixture. The reaction mixture was stirred at room temperature for 1.5 hours and quenched with a saturated solution of NH_4Cl (40 mL). The organic layer was extracted with EtOAc (2x20 mL) and washed with brine (4x20 mL). The organic layer was dried over $MgSO_4$, filtered, and concentrated under vacuum on a rotary evaporator to afford a yellow-orange oil. The crude oil was purified by column chromatography with 230-400 mesh silica gel and a 99:1 mixture of EtOAc:TEA as the eluant to afford the desired compound, **4** in a 82.3% yield (1.147 g) over two steps as a clear yellow oil. 1H NMR (400 MHz, CDCl3) δ 5.64 (m 1H), 5.50 (m, 1H), 4.11 (m, 1H), 3.68 (m, 2H), 3.41 (qt, J = 3.6 Hz, 1H), 2.21 (dt, J = 6.8, 1.6 Hz, 1H), 2.04 (m, 2H), 1.79 (m, 1H), 1.65 (m, 2H), 1.33 (m, 5H), 0.89 (m, 3H).

2.2.4 *(2S,3R)-2-((R)-1-iodopentyl)tetrahydro-2H-pyran-3-ol (**5**)*: To an oven dried 100 mL round bottom flask equipped with metallic stirbar under argon, **4** (0.5 g, 2.90 mmol, 1.0 equiv) was taken in dry THF (40 mL) and cooled to 0°C in an ice-water bath. Iodine (2.211 g, 8.71 mmol, 3.0 equiv) and sodium bicarbonate (0.732 g, 8.71 mmol, 3.0 equiv) were added and the reaction mixture was stirred at -10°C overnight in an acetone bath cooled by the NESLAB CC-100 Cryostat. The reaction mixture was warmed and stirred at room temperature for 6 hours and then quenched with a saturated aqueous solution of sodium thiosulfate (20 mL). The organic layer was extracted with EtOAc (2x20 mL) and washed with brine (3x20 mL). The organic layer was dried over $MgSO_4$, filtered, and concentrated under vacuum on a rotary evaporator to afford a clear oil. The crude oil was purified by column chromatography with 230-400 mesh silica gel and a 7:3 mixture of hexanes:EtOAc as the eluant to

afford the desired compound, **5** in a 54.1% yield (0.4612 g) as a clear yellow oil. ^{1}H NMR (400 MHz, $CDCl_3$) δ 3.48 (d, *J*=2.4 Hz 1H), 3.40 (dt, *J*=10.0, 0.8 Hz 1H), 3.99 (dd, *J* = 11.2, 4.8 Hz 2H), 3.42 (dt, *J* = 10.0, 0.8 Hz), 2.00-1.20 (m, 8H), 0.91 (t, *J* = 5.2 Hz, 3H).

2.2.5 *(2S,3R)-2-((S)-1-iodopentyl)tetrahydro-2H-pyran-3-yl acetate (**10**)*: To an oven dried 50 mL round bottom flask equipped with magnetic stirbar under argon, **5** (45.5 mg, 0.153 mmol, 1.0 equiv), Ac_2O (312 mg, 3.06 mmol, 20.0 equiv) and pyridine (121 mg, 1.53 mmol, 10.0 equiv) were taken in dry CH_2Cl_2 (20 mL). The reaction mixture was stirred overnight at room temperature. DMAP (0.0768 g, 0.628 mmol, 4.1 equiv) was added and the reaction mixture was stirred overnight at room temperature. The reaction mixture was quenched with a saturated aqueous sodium bicarbonate solution (10 mL). The organic layer was extracted with Et_2O and washed with a saturated aqueous $CuSO_4$ solution (2x15 mL) and brine (2x15 mL). The organic layer was dried over $MgSO_4$, filtered, and concentrated under vacuum on a rotary evaporator to afford an orange-yellow oil. The crude oil was purified by column chromatography with 230-400 mesh silica gel and a 9:1 mixture of hexanes:EtOAc as the eluant to afford the desired compound, **10** in a 65.6% yield (0.0341 g) as an orange-yellow oil. ^{1}H NMR (400 MHz, $CDCl_3$) δ 4.81 (dt, *J* = 8.0, 4.0 Hz, 1H), 4.64 (dd, *J* = 8.0, 4.0 Hz, 1H), 4.44 (dd, *J* = 8.0, 4.0 Hz, 1H), 3.76 (dt, *J* = 8.0, 4.0 Hz, 1H), 3.54 (dd, *J* = 8.0, 4.0 Hz, 1H), 2.05 (s, 3H), 2.00-1.20 (m, 8H), 0.91 (t, *J* = 5.2 Hz, 3H).

2.2.6 *(2R,3R)-2-pentyltetrahydro-2H-pyran-3-yl acetate* **(11)**: To an oven dried 50 mL round bottom flask equipped with magnetic stirbar under argon, compound **10** (0.2507 g, 0.737 mmol, 1.0 equiv) as taken in dry toluene (25 mL). Tributyltinhydride (0.429 g, 1.47 mmol, 2.0 equiv) and AIBN (0.0024 g, 0.015 mmol, 0.02 equiv) were added to the reaction mixture and the system was heated at 80°C for 3.5 hours. The reaction mixture was quenched with saturated aqueous solution of KF and the organic layer was extracted with EtOAc (3x15 mL) and washed with deionized water (3x15 mL) and brine (15 mL). The organic layer was dried over $MgSO_4$, filtered, and concentrated under vacuum on a rotary

evaporator to afford a clear oil. The crude oil was purified by column chromatography with 230-400 mesh silica gel and a 5:95 mixture of hexanes:EtOAc as the eluant to afford the desired compound, **11** in a 46.7% yield (73.7 mg) as a clear oil.

3. Results and Discussion

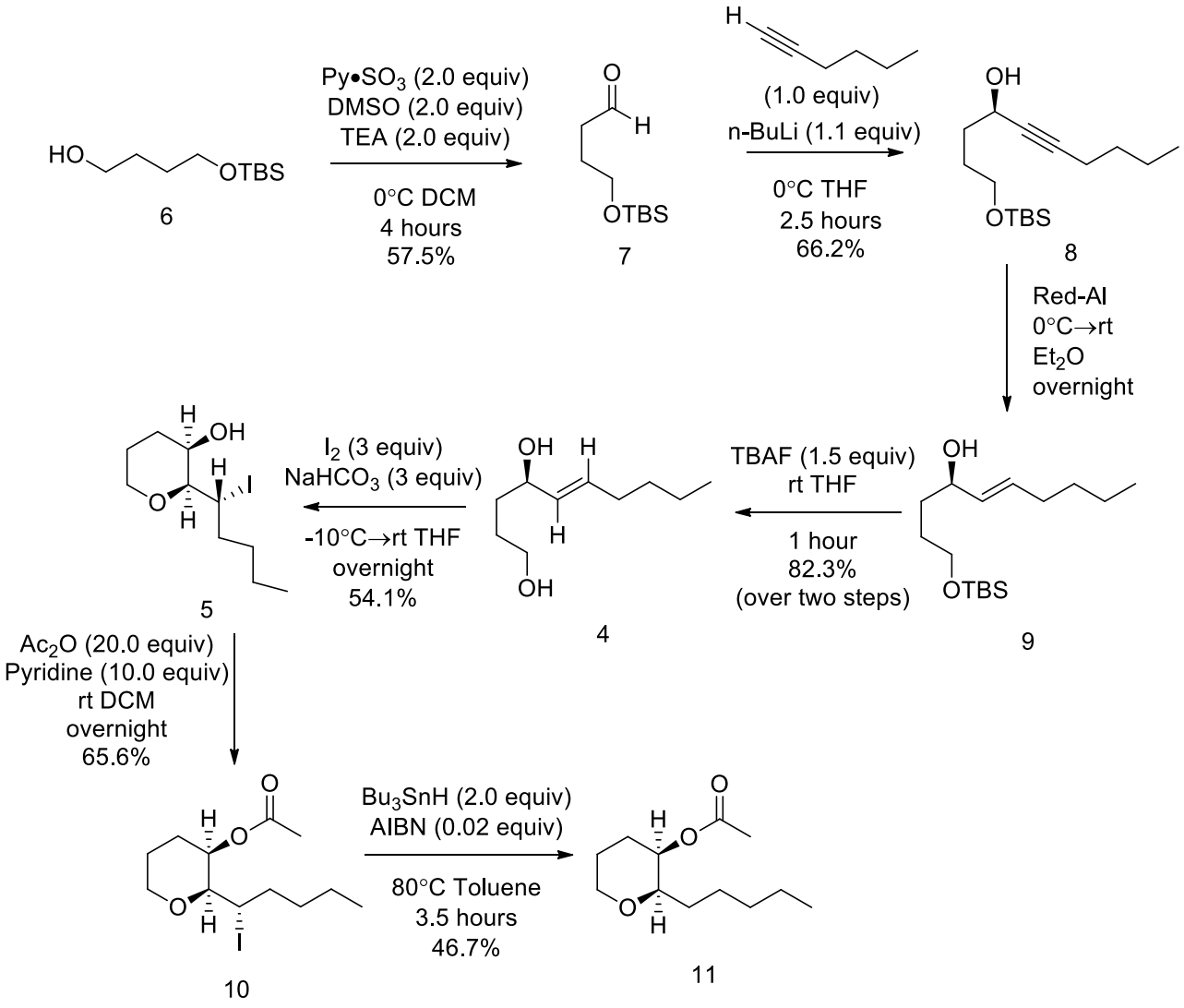

Scheme 4. The synthesis of an iodonium-activated cyclic ether model system

This project focused on the synthesis of E-alkenediol **4** to carry out the iodonium-activated cyclization to generate cyclic iodo-ether **5** as depicted in Scheme 4. Aldehyde **7** was generated using the Parikh-Doering oxidation of commercially available mono TBS-protected 1,4-butanediol **6** in moderate yields. The 1,2-addition of hexyne to aldehyde **7** afforded **8** without complications in moderate yields.

Difficulties were experienced during the $LiAlH_4$ reduction of the TBS-protected alkynyl butanediol **8,** as only starting material was recovered**.** The originally proposed $LiAlH_4$ reduction showed no conversion of the starting material. Since $LiAlH_4$ is a remarkably strong base and reductant, no conversion of the starting material through $LiAlH_4$ reductions suggest that the alkynyl diol **4** is too robust towards these conditions for the reaction to proceed. $LiAlH_4$ reduction was replaced with the hydroxyl-directed Vitride [Red-Al® sodium bis(2-methoxyethoxy)aluminum hydride solution 65% w/w in toluene] reduction, which provided the desired product as determined by ^{1}H NMR spectroscopy. The crude product **9** of the alkynyl reduction was carried over to deprotection of silyl ether, which afforded **4** in moderate yield over two steps. *E*-alkene **4** underwent iodonium-activated cyclization to give the cyclic iodo ether **5.** We believe that when the iodide is added to the alkene **4**, an iodo ether will form as the iodide will add in a Markovnikov orientation activating the alkene. The terminal alcohol will then add to the electrophilic alkene and form the ring. The activation of the allylic alcohol will result in an iodonium bridge, activating the beta carbon from the alcohol, resulting in a cyclized ether with a *trans-syn-trans* stereochemistry. The proposed mechanism is shown in Figure 7.

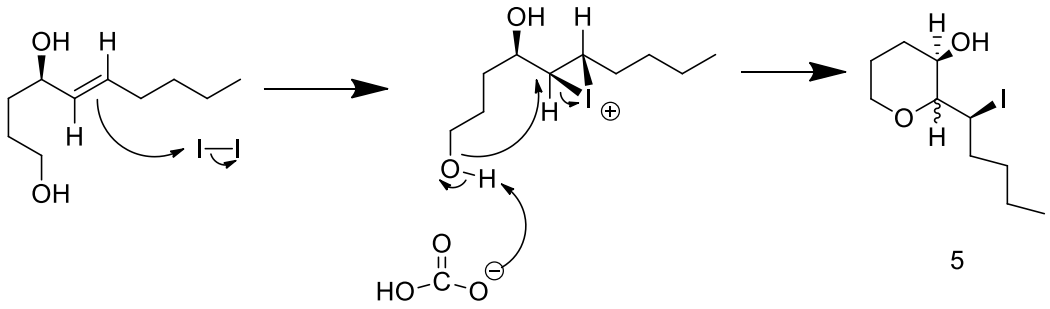

Figure 10. Proposed mechanism of cyclization by iodonium-activated hydroxyalkenes

The ^{1}H NMR data supported the generation of the *cis*-hydrogen stereochemistry at the ether ring juncture. The hydrogen adjacent to the ether along the ring juncture appeared as a doublet around 3.40 ppm (J=10.0 Hz, 0.8 Hz). This proton is relatively shielded, appearing up field on the spectrum congruent with an axial conformation at the ring juncture. A doublet of triplets appeared around 4.23

ppm (*J*=10.0 Hz, 3.2 Hz). The chair formation of the cyclic ether product with designated hydrogens and associated chemical shifts are shown in Figure 8. Relatively deshielded, appearing downfield on the spectra is congruent with an equatorial conformation along the ring juncture. Acetylation at the alcohol position further aided in structure elucidation by deshielding the hydrogens along the ring juncture in compound **10.** The broad peak that shifted to 5.37 ppm for the cyclic ether acetate product **10** was interpreted as a doublet of doublets with significant overlap. This downfield shift is characteristic of the beta-hydrogen of the ring juncture. The deshielded nature of this group is congruent with both acetylation effect and the equatorial configuration suggesting the cis-conformation of the hydrogens along the cyclic ether acetate **11**. Iodonium-bridge activated cyclization of E-alkenes afforded *trans-anti-trans* stereochemistry, an isomer of the desired *trans-syn-trans* stereochemistry of the brevetoxins.

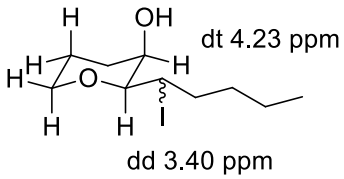

Figure 11. The chair formation of the cyclic ether product 10.

4. Conclusions and Future Studies

A seven-step synthesis was utilized to obtain chiral cyclic ethers cyclized through iodonium-bridge activation. Cyclic ether **10** served as a model system aimed to mimic the well-known *trans-syn-trans* configuration of the brevetoxin family. Structure elucidation and stereochemical assignment show that through iodonium-bridge activation, the cyclization of E-alkenediols afforded the *trans-anti-trans* stereochemistry, a stereoisomer of our target. Future studies should include cyclization studies with the Z-alkenediol. Starting with the opposite conformation initially might afford the desired stereochemistry when cyclization occurs. When iodine coordinates to the alkene to form the iodonium-bridge, the angle of entry might change with a cis-alkene, favoring ultimate formation of the *trans-syn-trans* stereochemistry. Alternative cyclization methods might also want to be explored such as mercury-

promoted cyclizations or ring closing metathesis reactions. This study was able to offer value characterization of iodonium-bridge catalyzed cyclizations. This information builds upon an ever-growing foundation aimed at efficient total synthesis of the brevetoxin family.

II. *Endo*-Selective Alkynol Cycloisomerization: Utilization of One-carbon Homologation to Synthesize Seven-membered Ring Glycals

1. Introduction

Septanoses are seven-membered ring carbohydrates that are structural derivatives of pyranoses, the naturally occurring six-membered sugar rings. These septanose carbohydrates are similar to naturally occurring carbohydrates and have demonstrated unique biological behavior under physiological conditions. Structurally related to the homologated versions of nucleic acids and protein monomers, these compounds serve as potentially useful in a number of physical, chemical, material and biological applications[14]. The size-expansion and ring oligomerization of natural biopolymers such as carbohydrates, proteins, and nucleic acids have yielded a number of structures capable of biological activity. Oligomers of these unnatural biopolymers can create complex unnatural structures that show predictable biological activity[14]. Developing the synthesis and combination of these septanose glycals can be directly applied to novel biological and material polymers[15]. These molecules show great promise in both biological and materials contexts so developing a reliable and effective synthesis can help understand the utility of these compounds.

There are multiple methods to access the unusual monosaccharide septanoses: cyclizations via C-O bond formation, reactions of carbohydrate-based oxepines, ring-closing metathesis, and cycloisomerization reactions. A common strategy in synthesizing septanoses is the cyclizations of the 6-hydroxyl group onto the aldehyde. The route generally entails the selective protection of the 6-hydroxyl group of the pyranose, followed by the protecting the hydroxyl groups and the protecting the aldehyde as an acetal. Micheel et al[16,17] reported the first synthesis of a septanose from galactose[15] (Scheme 5).

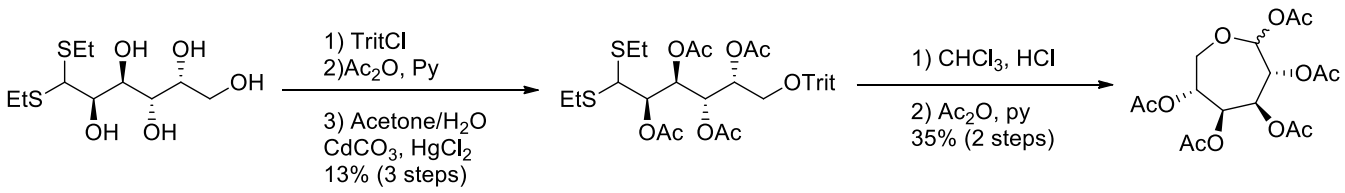

Scheme 5. Micheel's Synthesis of a Galactose-based Septanose[16]

Initial synthesis by Micheel et al garnered a relatively low yielding synthesis of the septanose. After the initial synthesis, Micheel had modified the synthesis, starting from the dithioacetal galactose derivative, where the acylation step was excluded from the overall synthesis[17]. In the modified synthesis, it is worth noting the acylation of the aldehyde, which suggests the septanose form is favored over the aldehyde open chain form[15].

From the mid-1970s to the 2000s, Stevens et al[20] utilized D-glucose as a base to synthesize their septanoses. Their synthesis was a one-step reaction in sulfuric acid and acetone to garner the diacetal septanose (Scheme 6). Following the first synthesis, Stevens et al added methanol to the reaction condition to generate the methylated α and β anomers[20].

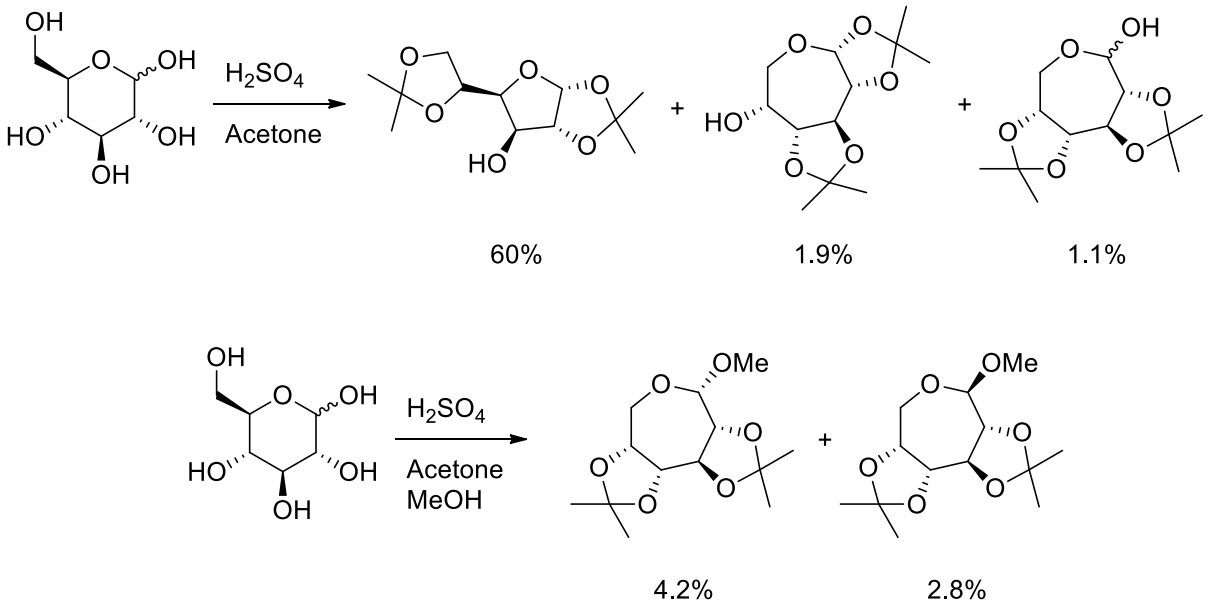

Scheme 6. Acid catalyzed one-step diacetal protection

Another strategy in synthesizing septanoses are through cyclopropanations of a 6-membered ring with a ring expansion. Hoberg and coworkers[22] reported one of the first syntheses of the oxepines via cyclopropanation (Scheme 7).

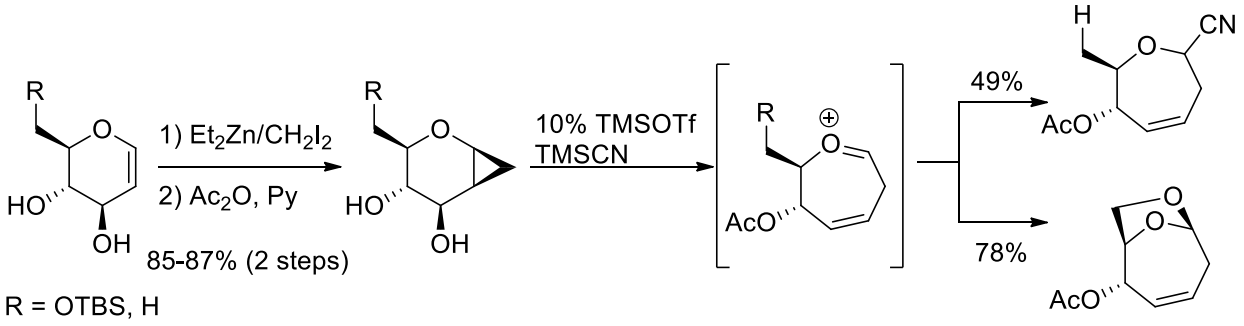

Scheme 7. Hoberg's synthesis of oxepines via cyclopropanation.[22]

Peczuh et al were able to synthesize their septanoses through the use of ring-closing metathesis with Schrock's catalyst (Scheme 8).

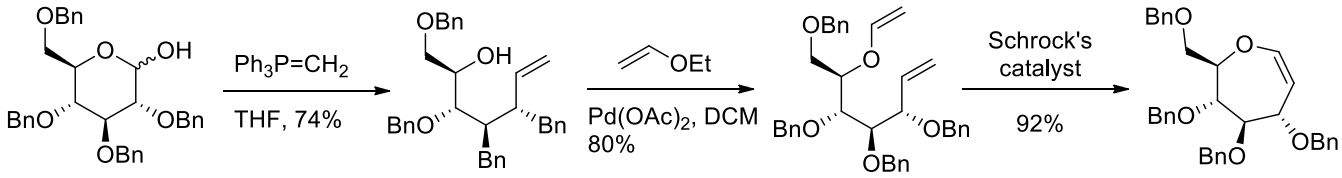

Scheme 8. Peczuh's synthesis of septanose glycals via Schrock's ring-closing metathesis[23]

This particular synthetic route is attractive due to its overall high yields for each step of the synthesis. However, in order to perform the ring-closing metathesis, Schrock's catalyst and palladium catalysts had to be used in order to form the desired septanose, a method which is neither cost effective nor practical in industrial production.

A particularly attractive route would be the cycloisomerization from alkynyl alcohols, where in the presence of tungsten catalysts would generate the cyclic ethers[24]. This reaction type is commonly used in a number of syntheses and preparations of biologically active species such as cyclic ether and polysaccharide structures because of its tolerance to varying functional groups[23]. Shown in Figure 9, the alkynyl alcohol coordinates with a metal catalyst to form a metal vinylidene. The vinylidene

intermediate cyclizes through a 1,2-migration of the terminal alkyne hydrogen. The transition can result in either the formation to a cyclic metal oxacarbene or a one-step transition to the cyclic enol ether[23].

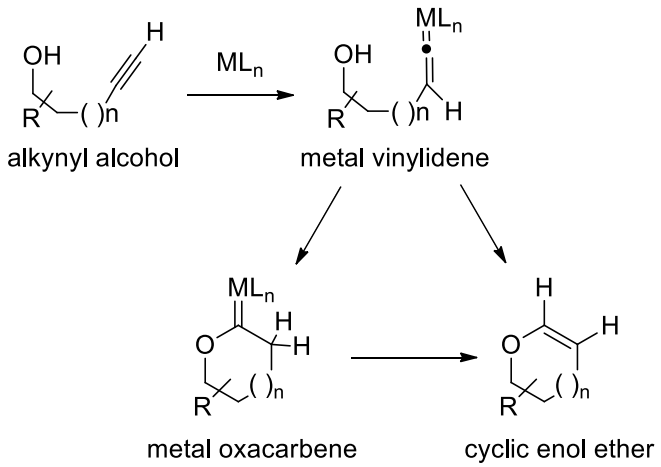

Figure 12. Metal-catalyzed alkynyl alcohol cyclizations

. Previous biological studies have been conducted on the polymers of various septanose carbohydrates, such as compound **15**. Di- and trisaccharide sugar chains were synthesized and subjected to jack bean α-mannosidase-catalyzed hydrolysis[26]. None of the examined mannoseptanosides showed inhibition of PNP-Man hydrolysis suggesting that seven-member sugar rings do not interact with the α-mannosidase hydrolytic enzymes[26]. Preliminary studies have shown the value of these biopolymers as biologically benign yet stable compounds. These compounds could be used as slow-dissolving medicinal materials, with degradation products producing innocuous sugar compounds easily metabolized within the body. These mannoseptanosides may show promise in the materials sciences as biological sutures and further studies should be conducted to accurately quantify the properties of these compounds.

The primary aim of this work focuses on synthesizing seven-membered ring glycals, specifically compound ***4***, from commercially available starting material. The proposed synthetic method is shown in Scheme 9 beginning with a one-carbon homologation of acetonide-protected D-(-)-ribose. Alkyne

formation will result from the Bestmann-Ohira modification of the Seyferth-Gilbert homologation with the anomeric isomer of the acetonide-protected ribofuranose **12**.

2. Experimental

2.1 General Experimental Procedures

All commercially available reagents were purchased from Sigma-Aldrich, Inc. and used without further purification. ^{1}H NMR studies used for structure elucidation were performed on the Varian INOVA 400 spectrometer at 400 MHz in $CDCl_3$, using the $CDCl_3$ singlet at 7.26 ppm as an internal reference. All reactions were conducted in oven-dried round bottom flasks under an inert argon atmosphere.

2.2.1 (3aR,6R,6aR)-6-(hydroxymethyl)-2,2-dimethyltetrahydrofuro[3,4-d][1,3]dioxol-4-ol (**12**)[27]: To two separate 500 mL round bottom flasks equipped with metallic stirbars under argon, D-(-)-ribose (10.0 g, 66.6 mmol, 1.0 equiv) was dissolved in acetone (200 mL) at room temperature. Catalytic amounts of H_2SO_4 (1 mL) was added dropwise until complete consumption of originally insoluble starting material. Both reaction mixtures were stirred for 1.5 hours and neutralized with excess solid sodium bicarbonate. The reaction mixtures were filtered of excess sodium bicarbonate and concentrated under vacuum on a rotary evaporator to afford colorless crude oils. The two crude oils were combined and purified by column chromatography with 230-400 mesh silica gel and a 1:1 mixture of hexanes:EtOAc as the eluant to afford the desired compound, (3aR,6R,6aR)-6-(hydroxymethyl)-2,2-dimethyltetrahydrofuro[3,4-d][1,3]dioxol-4-ol in a 55.77% yield (14.1274 g) as a yellow oil. ^{1}H NMR (300 MHz, $CDCl_3$) δ 5.42 (d, J =6.6 Hz, 1H), 4.85 (d, J = 6.3 Hz, 1H), 4.59 (d, J = 6.3 Hz, 1H), 4.42 (m, 1H), 3.73 (d, J = 2.7 Hz, 2H)

2.2.2 Dimethyl (2-oxopropyl)phosphonate (**17**)[28]: To an oven dried 2 liter round bottom flask equipped with metallic stir bar under argon, chloroacetone (100.0 g, 1080 mmol, 1 equiv) was taken in a **4:5** solution of acetone:acetonitrile and KI (179.8 g, 1080 mmol, 1 equiv) at room temperature. The yellow reaction mixture was stirred for an hour and trimethyl phosphite (134.0 g, 1080 mmol, 1 equiv)

was added to the reaction mixture in 20 mL portions. The yellow reaction mixture turned white upon trimethyl phosphite addition and the reaction mixture was stirred overnight at room temperature. The reaction mixture was then heated in a 50°C oil bath for six hours. A color change from a white to yellow-orange solution was observed and the reaction was probed by TLC for completion. The reaction mixture was cooled to room temperature and the precipitate was separated by vacuum filtration with a water aspirator through a pad of Celite. The crude filtrate was evaporated under vacuum on a rotary evaporator. ***Warning: evaporation should occur in a fume hood to avoid iodomethane exposure.*** The crude mixture was purified by vacuum short path distillation (path length). The distillation was performed in a 175°C oil bath at 0.3 Torr. The desired compound distilled as the third fraction with a boiling point at 130°C. Dimethyl (2-oxopropyl)phosphonate was obtained in a 51% yield (**92.0407** g) as a bright yellow oil. ^{1}H NMR (400 MHz, $CDCl_3$) δ 3.78 (d, *J* = 11.4 Hz, 6H), 3.09 (d, *J* = 22.8 Hz, 2H), 2.32 (s, 3H).

2.2.3 Dimethyl (1-diazo-2-oxopropyl)phosphonate (**13**)[28]: To a dry 1 L round bottom flask under argon equipped with mechanical stirrer at moderate stirring speed controlled by a Variac gauge, compound **17** (5.0 g, 30.1 mmol, 1 equiv) was taken in 30.1 mL of dry toluene and cool to 0°C. NaH (1.08 g (NaH only), 1.8 g (60% mineral oil dispersion) 45.2 mmol, 1.5 equiv) was added to the reaction mixture in three portions. Upon NaH addition, the clear yellow reaction mixture became an extremely viscous opaque white yellow mixture that was difficult to stir. The reaction mixture was stirred for an hour to allow H_2 evolution to occur. *p*-ABSA (7.23 g, 30.1 mmol, 1 equiv) was taken in 10.1 mL of dry THF and added dropwise to the reaction mixture. The reaction mixture was maintained at 0°C overnight using the NESLAB CC-100 Cryostat. After stirring, the reaction mixture was diluted with petroleum ether (100 mL) and filtered through a pad of Celite. The filter was rinsed multiple times with Et_2O (5x50 mL) and the crude mixture was concentrated under reduced pressure on a rotary evaporator. The crude oil was purified by column chromatography with 230-400 mesh silica gel and a 1:1 mixture of

hexanes:EtOAc as the eluant to afford the desired compound, **13** in a 34% yield (1.9544 g) as a bright yellow oil. ^{1}H NMR (400 MHz, $CDCl_3$) δ 2.25 (s, 3H), 3.09 (d, *J* = 22.8 Hz, 2H), and 3.81 (d, *J*=11.6 Hz, 6H).

2.2.4 (R)-1-((4R,5S)-5-ethynyl-2,2-dimethyl-1,3-dioxolan-4-yl)ethane-1,2-diol: To an oven-dried 25 mL three-necked round bottom flask equipped with metallic stirbar, compound **12** (1.0 g, 5.25 mmol, 1 equiv) and K_2CO_3 (0.966 g, 6.99 mmol, 1.33 equiv) were taken in 6 mL of MeOH and brought to reflux. Diazo phosphonate **13** was taken in 5 mL of MeOH and added dropwise over 8 hours using a syringe pump. After addition of compound **13** the reaction mixture was cooled to room temperature and the excess K_2CO_3 precipitate was removed by filtration. The solution was neutralized with 10 mL of 1N HCl and the organic layer was extracted with EtOAc (3x15 mL) and washed with deionized water (3x15 mL). The organic layer was dried over $MgSO_4$, filtered, and concentrated under vacuum on a rotary evaporator to afford a viscous white oil. The crude oil was purified by column chromatography with 230-400 mesh silica gel and a 4:1 → 1:1 gradient elution of hexanes:EtOAc as the eluant to afford the desired compound, 10 in a 17.4% yield (0.1702 g) as a viscous white oil.

3. Results and discussion

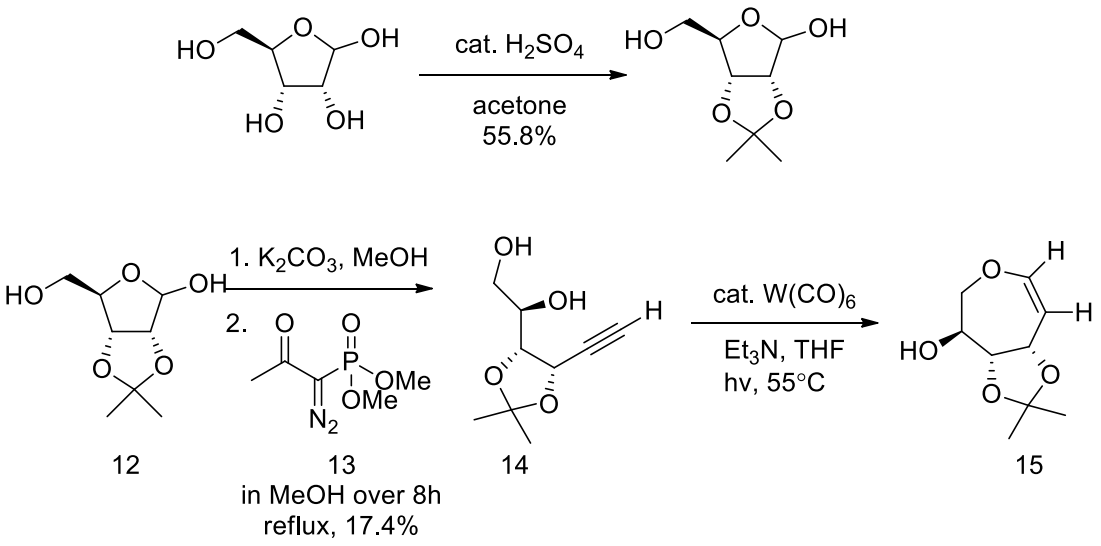

Scheme 9. Synthetic scheme for septanose glycal from D-(-)-ribose

Compound **12** was prepared by acetonide protection of D-(-)-ribose in moderate yield using a protocol described by Hughes et al[27]. Increases in reaction time can result in differential protection patterns, therefore the reaction was carefully monitored to ensure generation of the desired protection pattern within the product. Often, the crude material from acetonide protection used in subsequent reactions after thorough evaporation of solvents. A decrease in yield could have originated from column chromatography of this compound. In equilibrium with the opened chain form, the crude mixture can be separated into the two distinct anomeric isomers. The eluted fractions should be analyzed carefully through NMR to prevent loss of the desired product in the undesired anomeric form.

Compound **13**, widely known as the Bestmann-Ohira reagent, was generated through a two-step conversion from chloroacetone as shown in Scheme 3 reported by Pietruszka et al[28].

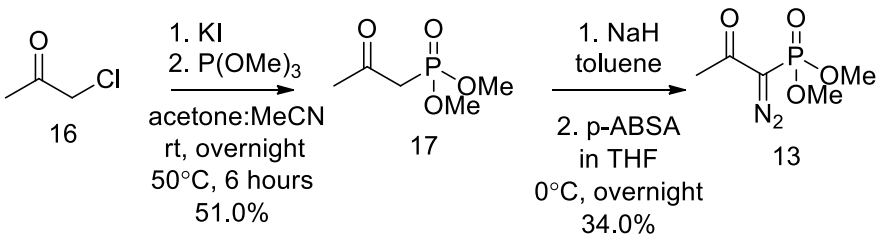

Scheme 10. Synthetic pathway for the Bestmann-Ohira reagent.

Conversion from **16** to **17** involved a Finkelstein halogen replacement and two concerted substitution reactions to carry out phosphonation as shown in Figure 10.

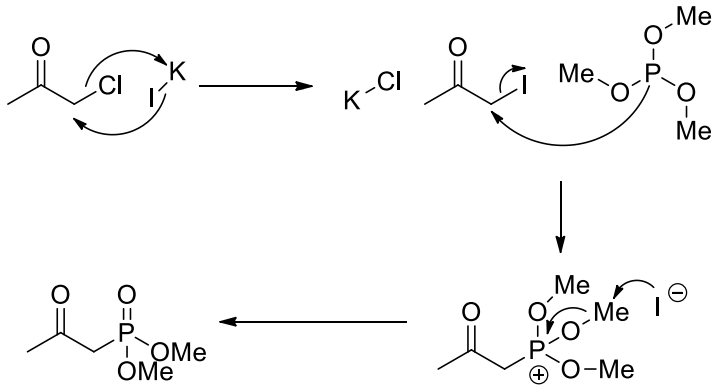

Figure 13. The mechanism for the phosphonation of chloroacetone.

Difficulties were experienced during the distillation of the product from the crude reaction mixture. Besides temperature and pressure deviation from the literature values, the reaction mixture showed poor separation of the desired phosphonate **17** with a side product generated within the system. After varying the temperature and pressure of the system, distillation succeeded when the system was subjected to an oil bath at 175°C under a vacuum at 0.3 Torr with the desired product eluting in the third fraction. The distillation apparatus included an 8.0 cm long path condenser. The observed boiling point was at 130°C, a large deviation from literature reported 69-70°C (0.47 mbar) and 85-88°C (0.67 mbar). Because of poor separation, some of the phosphonate product **17** was lost during distillation. For better separation, a Vigreux distillation column should be used to increase the number of theoretical plates extending the vapor path length.

Compound **17** was converted to **13** through NaH deprotonation and Regitz diazo transfer with *p*-ABSA as shown in Figure 11.

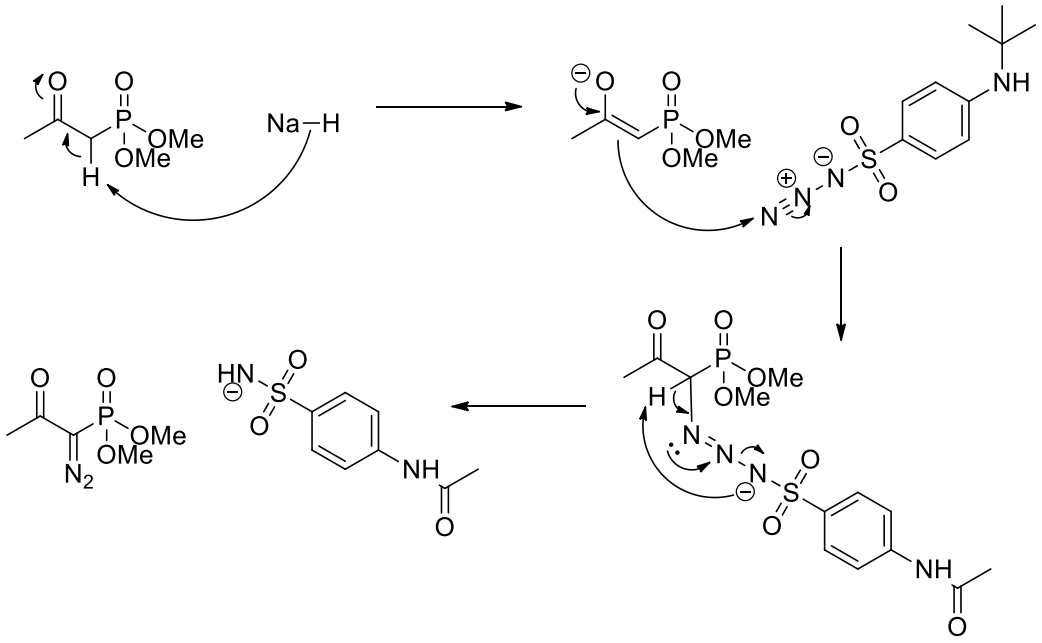

Figure 14. Mechanism for NaH deprotonation and Regitz diazo transfer to generate diazo phosphonate 13.

The reaction proceeded without any major problems and the work up was relatively straight forward. ^{1}H NMR analysis of the crude material showed completely conversion of starting material to the desired diazo phosphonate **13**.

Alkynyl diol **14** was synthesized by adding compound **13** to the acetonide ribofuranose **12** by using the Bestmann-Ohira modified Seyferth-Gilbert homologation (Figure 12).

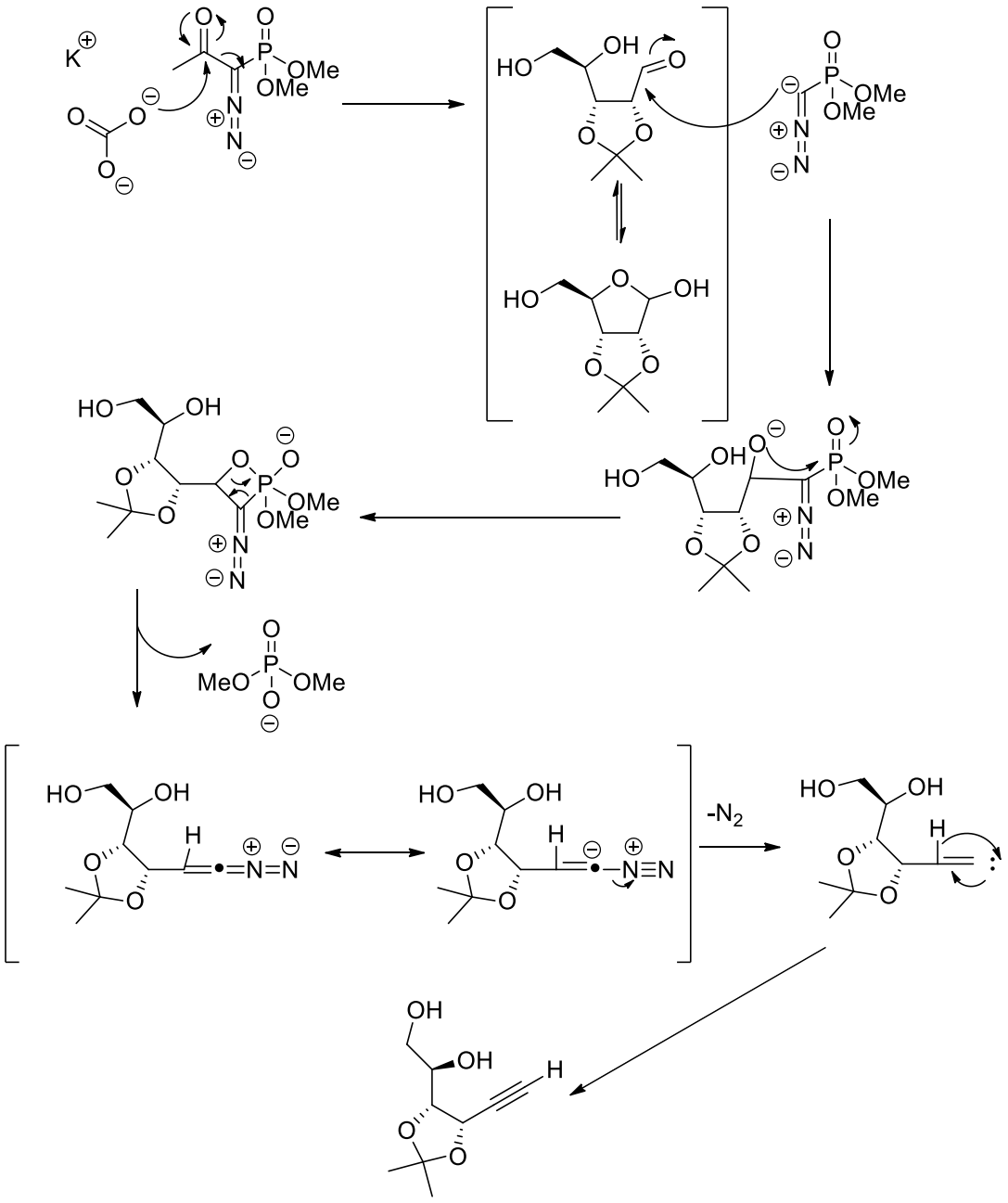

Figure 15. Tbe mechanism for the Bestmann-Ohira modification of the Seyferth-Gilbert Homologation.

Initially, problems with conversion were experienced due to the rate of addition for the Bestmann-Ohira reagent **13**. After multiple trials, it was verified that regardless of the reaction scale, reaction concentration should be maintained and the reagent should be added drop-wise over eight hours. Due to the highly polar nature of the compound, difficulties were experienced during purification and characterization of the compound. Purification required flash column chromatography (eluted with a 4:1

→ 1:1 gradient of hexanes:EtOAc) and extra care was taken to concentrate the sample under reduced pressure.

Due to purification difficulties, the cyclization reaction still needs to be explored to complete the synthesis of septanose glycal **15**. The next and final step of the synthesis requires $W(CO)_6$ catalyzed cyclization of the alkynyl diol **14**.

4. Conclusions and Future Studies

The major aim of this project involves developing a reproducible multi-gram scale organic synthesis preparation to generate septanose glycal **15** from commercially available D-(-)-ribose. Alkynyl diol **14** was synthesized and characterized from acetonide-protected D-(-)-ribose using the Bestmann-Ohira reagent **13**. Compound **13** was synthesized and characterized by a two-step conversion from chloroacetone. This project, thus far, has addressed a number of difficulties that are associated with reliably generating compounds **12-17**. Future studies should include scaling up the reaction and improving the overall yields of problematic steps. For instance, literature precedent has suggested TBS-protecting the acetonide ribofuranose **12** along with changing from K_2CO_3 to Cs_2CO_3 can significantly improve the yield of the homologation step[23].

III. Synthesis and Characterization of Monothiopyrophosphate: A Therapeutic Candidate for Inhibition of Vascular Calcification

1. Introduction

Cardiovascular calcification is described as the accumulation of apatite and other crystals in the intima and media layers of the blood vessel in native and bioprosthetic heart valves [29]. Vascular calcification is most commonly associated with atherosclerosis and advanced age. Generally caused by increased plaque calcification, coronary artery calcification is three to five times more prevalent in patients with chronic kidney disease (CKD) and end stage renal disease (ESRD)[30, 31, 32, 33]. In general, vascular calcification significantly increases the risk of morbidity and mortality due to cardiovascular disease in CKD and ESRD patients.[34]

Intimal calcification occurs in atherosclerosis patients with or without kidney disease whereas medial calcification occurs most often in patients with chronic renal failure or diabetes. In the absence of a preexisting condition such as diabetes or atherosclerosis, medial calcification can also occur in the elastin fibers of smooth muscles in patients afflicted with EKD and ESRD. The pathophysiology ranges largely in observed cases but all result in hydroxyapatite formation along the vasculature.[37]

Mechanistically, vascular calcification has two main origins: direct mineralization of the vascular extracellular matrix or cellular regulation. Direct mineralization can cause medial elastic calcification of the lamellae but is commonly avoided by the presence of inhibitory proteins such as the matrix Gla protein (MGP).[35] Cell-regulated vascular calcification originates from impaired mineral metabolism which transforms vascular smooth muscle cells into chondroblast and osteoblast-like cells. In normal vascular cells, inorganic pyrophosphate acts as an inhibitor of hydroxyapatite formation. Within these cells, the tissue-nonspecific alkaline phosphatase (TNAP) activity is low, leaving abundant concentrations of pyrophosphate present to inhibit extracellular matrix mineralization.[36] In osteoblast/osteocyte bone cells, high TNAP activity hydrolyzes inhibitory pyrophosphate into units of

inorganic phosphate. The accumulation of these inorganic minerals within the extracellular matrix contributes to vascular calcification. CKD and ESRD patients are intimately linked with these insoluble mineral depositions because of impaired mineral metabolism originating from renal impairment[36]. In uremic patients, mineral metabolism is disrupted and these vascular cells are transdifferentiated into chondroblast and osteoblast-like cells with higher TNAP activity as shown in Figure 13.

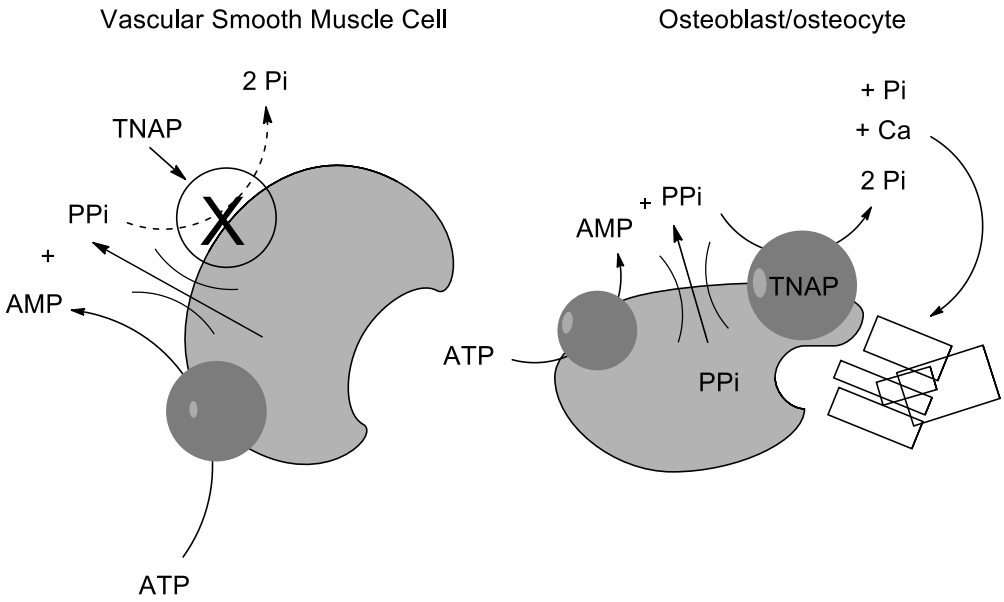

Figure 16. The central role that TNAP plays within vascular smooth muscle and osteoblast/osteocyte cells[37]

High TNAP activity will hydrolyze the inhibitory pyrophosphate within the cell, initiating the mineralization process by formation of hydroxyapatite.[37] Transformation of these cells also triggers the production of matrix vesicles, transcription factors, and a number of other mediators associated with dental and skeletal development that assist in the mineralization process. The abundance of these mineralization factors increases the abundance of free-circulating calcium and phosphate, decreasing inhibitory mechanisms such as MGP activity, pyrophosphate concentrations, and other inhibitors such as fetuin-A and ultimately results in vascular calcification.[37]

On a molecular level, vascular calcification results from the deposition of insoluble hydroxyapatite (HA), $Ca_{10}(PO_4)_6(OH)_2$, formed from free calcium and phosphate ions within vessels and

vasculature. The physical chemistry of HA formation exceeds simple first order precipitation of calcium ions and inorganic phosphate. Formation happens in two steps, as shown in Figure 14.

Figure 17. The two step formation of hydroxyapatite from calcium and inorganic phosphate.[35]

Initially, free-flowing calcium and inorganic phosphate within the blood plasma forms into an insoluble solid amorphous crystalline hydrate, $CaHPO_4 \bullet H_2O$. The rate of formation of $CaHPO_4 \bullet H_2O$ is particularly low ($K_{sp} = 2.3x10^{-7}\ M^2$) at physiological pH (7.4) and temperature (37°C) and is in equilibrium with dissociation into its soluble components. After formation of the $CaHPO_4 \bullet H_2O$, however, HA can be formed directly from spontaneous and irreversible hydrolysis at physiological conditions. Vascular calcification due to renal failure is predominantly is caused by a disruption of cellular inhibitory pathways of hydroxyapatite formation. Key physiological inhibitors include control of PPi concentrations and the presence of Matrix Gla protein (MGP). Uremic vessels have a higher rate of pyrophosphate hydrolysis due to increased alkaline phosphatase activity.[37] Alkalemia in hemodialysis patients favors hydroxyapatite formation and decreased carboxylation of MGP inactivating and suppressing inhibitory activity, further increasing vascular calcification of the blood vessels.[37]

Previous studies have yielded preliminary data that has indicated thiopyrophosphate as an ideal therapeutic candidate for controlled inhibition of hydroxyapatite formation. Other candidates previously explored are bisphosphonates, pyrophosphate, polyphosphates, phosphocitrate and thiosulfate. Initially, bisphosphonates were believed to be the ideal therapeutic candidate. Not only are these pyrophosphate analogs nonhydrolyzable, they were shown to be potent inhibitors in both *in vitro* and *in vivo* studies credited to completely inhibit vascular calcification in uremic rats. The clinical applications of these candidates, however, are limited due to high dosage requirement and adverse over-suppression of bone formation.[44, 45, 46] Also, due to their robust nature, bisphosphonates have a long half-life and compound

elimination requires renal clearance.[46] Pyrophosphate was an attractive candidate because it is an endogenous inhibitor that can effectively inhibit hydroxyapatite formation as seen with other bisphosphonates. Also, since pyrophosphate is naturally hydrolyzable by TNAP, bone formation was not altered in the presence of pyrophosphate. The short half-life of pyrophosphate *in vivo*, however, required a high dosage that commonly resulted in peritoneal inflammation.[47]

Polyphosphates were explored because of their commercial accessibility and their common usage as a food additive. Their conjugated polymer nature could have a prolonged effect due to the continual generation of pyrophosphate during metabolism. Hydroxyapatite formation and alkaline phosphatase assay showed complete inhibition of vascular calcification while *in vivo* studies showed no effect on calcium levels. Phosphocitrate and thiosulfate were also considered as possible candidates. Phosphocitrate is known to inhibit hydroxyapatite formation while still being susceptible to hydrolysis, proving to be a potent inhibitor *in vitro*. Clinical studies have shown that thiosulfate prevents nephrolithiasis in patients and reduces tumoral calcification due to renal failure.[48] Clinical and anecdotal evidence credit thiosulfate as an effective inhibitor for arteriolopathy and calcification[41,42,43]. *In vivo* studies in uremic rats, however, showed that high doses were required and bone formation was also compromised. *In vitro* studies also showed that hydroxyapatite formation was not effected by thiosulfate. This candidate most likely affects a different cellular mechanism responsible for calcification which eliminates it as a viable candidate.[43]

First and foremost, this project is aimed to synthesize and characterize monothiopyrophosphate. Commercially available sodium thiophosphate will be heated in an environment devoid of moisture to generate monothiopyrophosphate mixed with pyrophosphate and H_2S as shown in Scheme 11. The project will test this compound in a number of *in vitro* and *in vivo* assays to test for hydrolytic nature, ability to inhibit hydroxyapatite formation, dosage requirements and practicality as a therapeutic.

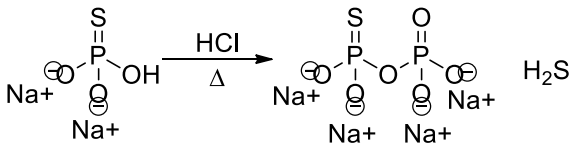

Scheme 11. The proposed synthesis of monothiopyrophosphate by pyrolysis.

2. Experimental

2.1 Monothiopyrophosphate[50]: To a small reaction vial, thiophosphate (SP_i) (0.50 g, 2.78 mmol, 1.0 equiv) was dissolved in a minimal amount of deionized water. A calibrated Hanna Instruments Hi 98103 Checker Ph Tester was used to measure the pH of the solution. The reaction mixture was adjusted to thiophosphate's first titration point (pH 10.2) with concentrated HCl. The water in the reaction mixture was removed under vacuum using a rotary evaporator. Separately, a dry flat-bottomed flask was filled with around 2 cm (depth) of P_2O_5. Copper wire was wrapped around the reaction vial (to prevent the vial from falling over within the flask) and the reaction vial was lowered into the flat-bottomed flask. The reaction vial was placed directly on top of the P_2O_5 layer. A glass adaptor was used to connect the apparatus to a vacuum and the reaction was dried for 6 hours at room temperature under vacuum (0.36 Torr). Every two hours, a butane torch was used to remove additional moisture on the exterior of the apparatus to ensure complete removal of water within the system. Extra care should be taken to void the reaction apparatus of all moisture. After drying, the apparatus was placed in an oil bath and the reaction mixture was heated at 153°C under vacuum for 2 hours. After heating, the apparatus was deconstructed, the reaction vial was removed from the flat-bottomed flask and the P_2O_5 was quenched in a basin of ice water. The crude solid was solvated in D_2O and analyzed by ^{31}P NMR. Crude spectroscopic data shows ^{31}P NMR (162 MHz, $CDCl_3$) δ 37.41 ppm (d, J = 28.00 Hz, 1P), -10.589 (d, J = 28.00 Hz, 1P) at pH 4.8.

3. Results and Discussion

Synthesis and characterization of the monothiopyrophosphate (SPP_i) proved to be difficult. The protocol used initially drew from the reported synthesis and characterization developed by Dunaway-Mariano et al for monothiopyrophosphate[49]. ^{31}P NMR was used to characterize the crude material and subsequent

purification attempts however the data did not support the synthesis of our desired compound. An alternative reported synthesis was used with increased drying time and reaction temperature. The crude material was analyzed and ^{31}P NMR studies strongly support the synthesis of our desired compound. The 31P NMR was conducted in basic and acidic conditions and are shown in Figure 15 and Figure 16 respectively. Current efforts are being taken to purify and characterize the crude thiopyrophosphate so further biological studies of this therapeutic candidate can be explored.

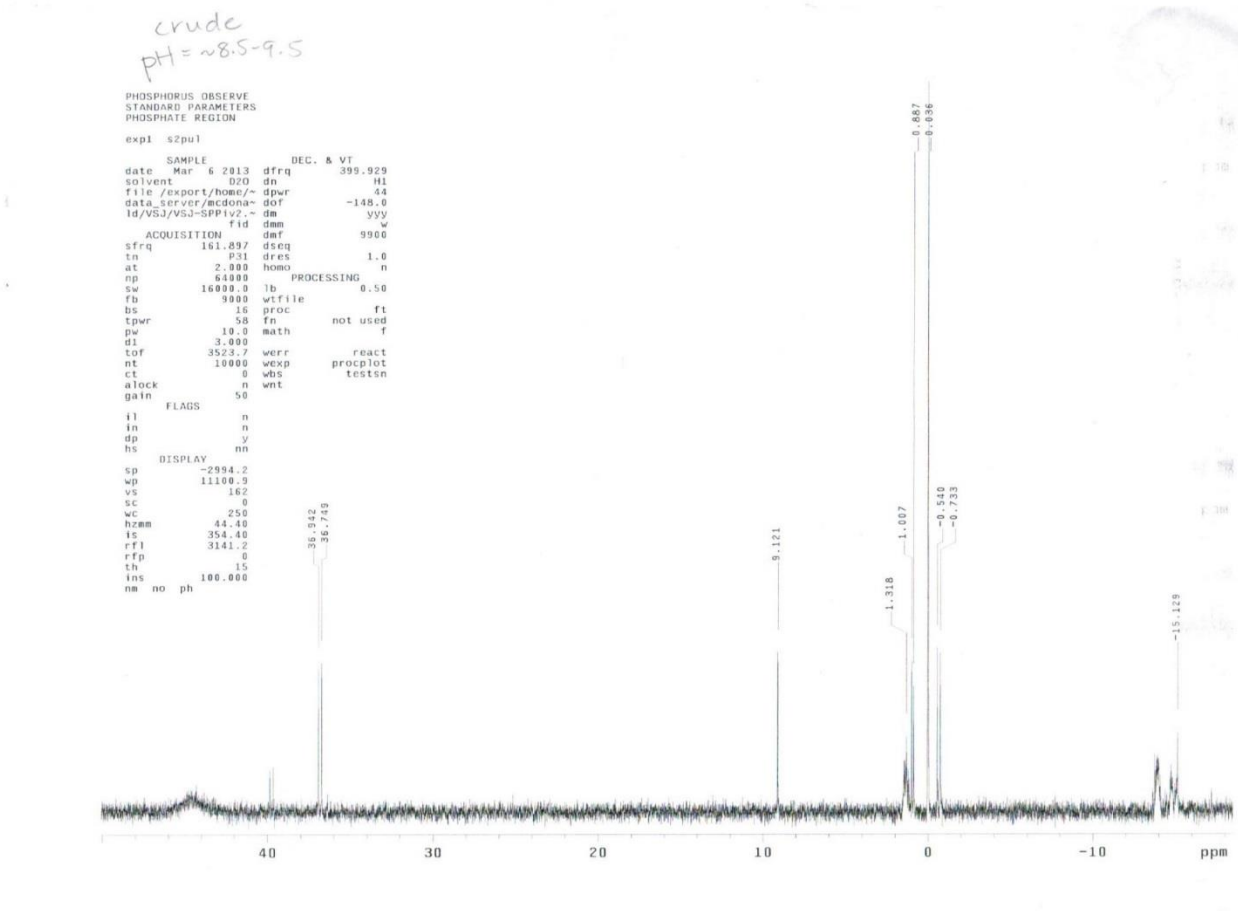

Figure 18. ^{31}P NMR of crude SPP_i product in basic conditions.

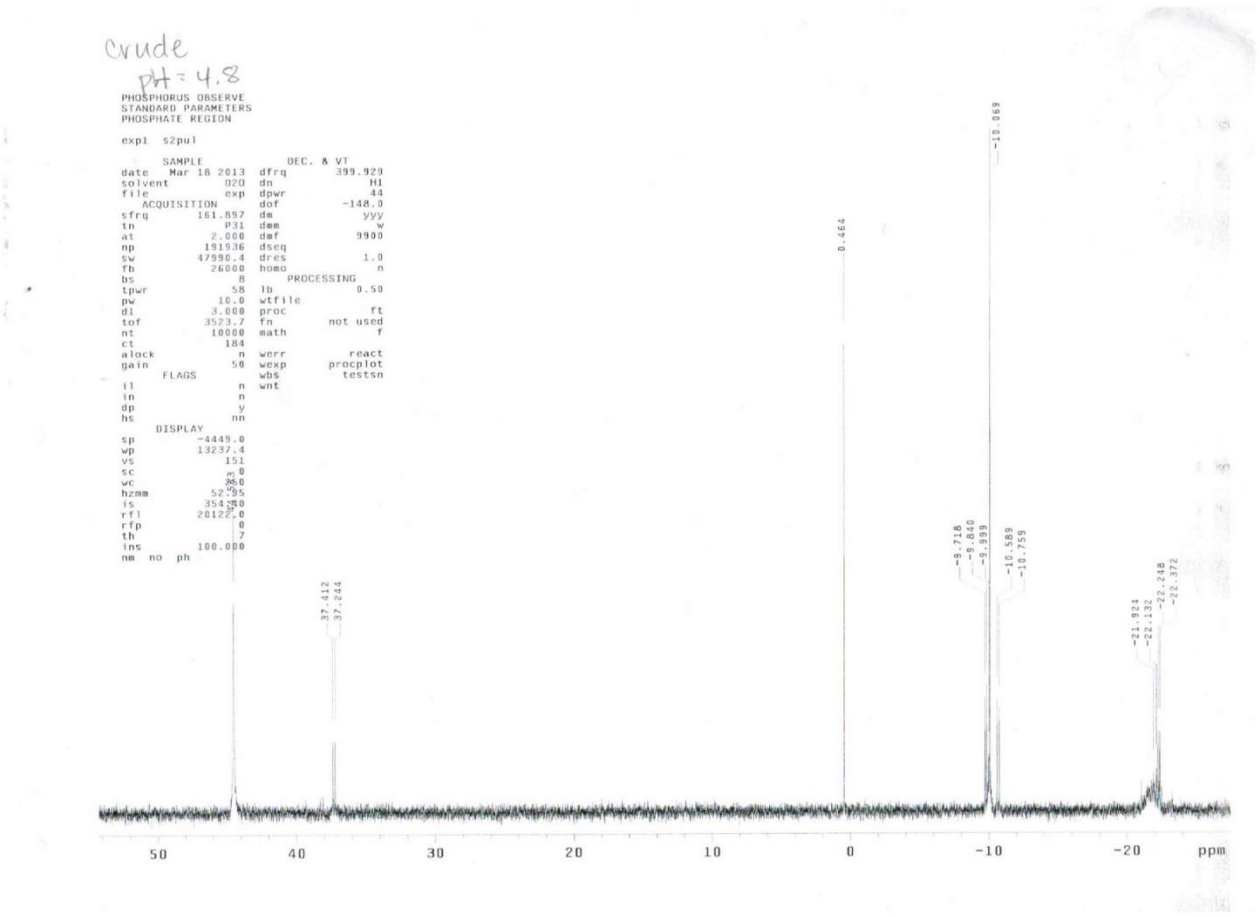

Figure 19. ^{31}P NMR of crude SPP_i product at pH 4.8

The protocol started with titrating the pH of the starting material to a pH of 10.2, the first titration point, with concentrated HCl. The reaction mixture was evaporated *in vacuo* on a rotary evaporator. The reaction mixture was then placed in a drying apparatus over P_2O_5 (as described in the experimental) and dried *in vacuo* for three hours followed by heating at 110°C *in vacuo* for four hours. Dunaway-Mariano[49] reported that their modified procedure produced low to moderate yield of SPP_i characterized by a pair of doublets (d 34.0 ppm, and d -9.8 ppm, *J*=28 Hz) at pH 4.4. While the spectra didn't display the pair of doublets, deviation from the literature value was credited to the variation of ^{31}P NMR based on pH.

The substrate was eluted through a K_2CO_3 (0.2, 0.3…1.0 M) anion exchange column with Dowex 1x8 Cl resin and analyzed through the Fiske and Subbarow colorimetric phosphate assay [51]. The assay showed that the 0.2 M fraction had the presence of phosphate within and the fraction was analyzed by ^{31}P NMR. A standard column elution was conducted to verify the efficacy of K_2CO_3 as a liquid eluant with pyrophosphate and the starting material, thiophosphate (SP_i). Fiske and Subbarow analysis showed that SP_i eluted at 0.4/0.45M K_2CO_3 while the PP_i eluted at 0.1/0.15M K_2CO_3. This result shows that PP_i will elute before SP_i. While the results displayed a clean separation, early elution of PP_i turned our attention to other solvent systems such as HCl. Another standard column elution was conducted with Pi, PPi, and SPi as the compounds loaded. An alternative phosphate assay, developed by Dunham and Christianson, was used to analyze the eluted fractions. The P_i and PP_i eluted at 0.05M and 0.2M HCl respectively while the SP_i eluted at 0.15M. The standard column showed clean separation of these compounds with the HCl eluant system with the elution order as following: P_i, SP_i and PP_i. From this data, our desired product, SPP_i should in turn elute slightly after PP_i with the HCl ion exchange column.

Crude material was loaded and eluted through an HCl (0.05, 0.1…0.8M) column and the fractions were probed by the Fiske and Subbarow assay. Colorimetric determination showed that the 0.15M, 0.25M and 1M flush fractions contained the presence of phosphate and these samples were analyzed by NMR. At first glance, ^{31}P NMR of the 0.25M HCl fraction (**A**) showed two broad singlets with minute splitting that was promising in identification of pure thiopyrophosphate. While the splitting was unclear, the material was believed to be the desired product and was carried on to *in vitro* hydroxyapatite and hydrolytic phosphatase assays to determine the efficacy of this compound **A** within the physiological conditions.

The *in vitro* hydroxyapatite assay assessed the rate of hydroxyapatite formation at physiological conditions (pH 7.4, 37°C) over a twenty minute period. Comparing to the control standard, the obtained compound **A** inhibited hydroxyapatite formation, reducing the rate of formation two fold. The column

fractions were all subjected to an alkaline phosphatase assay that assessed the hydrolytic stability of the compound. In tandem with inorganic phosphatase, the Lin et al colorimetric phosphate assay of the fractions showed that the compound was susceptible to pyrophosphatase hydrolysis but resistant to calf intestinal alkaline phosphatase hydrolysis. In the smooth muscle lining of vasculature, TNAP, serves as the predominant pyrophosphate hydrolytic protein. With high TNAP activity within the cells, characteristic of patients with ESRD and vascular calcification, pyrophosphate derivatives will be rapidly hydrolyzed which partially accounts for the high dosage requirements of PP_i and other related analogues. With our obtained compound, resistance to TNAP hydrolysis can signify lower dosage requirements and long half-life within the body. The inorganic pyrophosphatase activity, however, shows that the compound **A** is still hydrolytically active and can be reduced to its phosphate components with ease within the body. Easy metabolism of these compounds is essential in patients already plagued with disruptions of their mineral metabolism such as patients with ESRD and increasing age. These *in vitro* assays show that the obtained compounds **A** is a promising therapeutic candidate because it is easily metabolized within the body but is robust within targeted cells.

After the *in vitro* studies, further NMR studies varying pH of known standard samples were conducted to address the ambiguity of the ^{31}P obtained for compound **A**. Originally, the broad splitting observed in was credited to the pH dependence of ^{31}P NMR. A pH dependent NMR study was conducted with two known standards of adenosine diphosphate (ADP) and PP_i at pH 4.4 and pH 8.5. ADP and PP_i were used as the standards because of their related nature to SPP_i. ADP was used as a positive control for the NMR experiments because ADP contains two non-equivalent phosphorus environments which would result in observable doublet splitting. ADP at pH 4.4 appeared as two broad doublets at -9.69 ppm and -10.68 ppm *(J*=19.59 Hz) as shown in Figure 15. At basic pH 8.5, ADP appeared as two broad doublets at -5.56 ppm and -10.025 ppm (*J*=22.02 Hz) as shown in Figure 16. PP_i was examined as a negative control because it has a close structural similarity to our desired compound.

Varying the pH of ADP showed that chemical shifts and coupling constants for ^{31}P NMRs are highly dependent on pH. Also, distinct doublet splitting was observed. The ADP experiment confirmed this result because it showed that if doublet splitting is present, it would be visible and apparent in the spectra. While the obtained compound **A** displayed promising *in vitro* activity, the absence of doublet splitting and associated coupling in the ^{31}P NMR were not consistent with the properties of the desired monothiopyrophosphate compound.

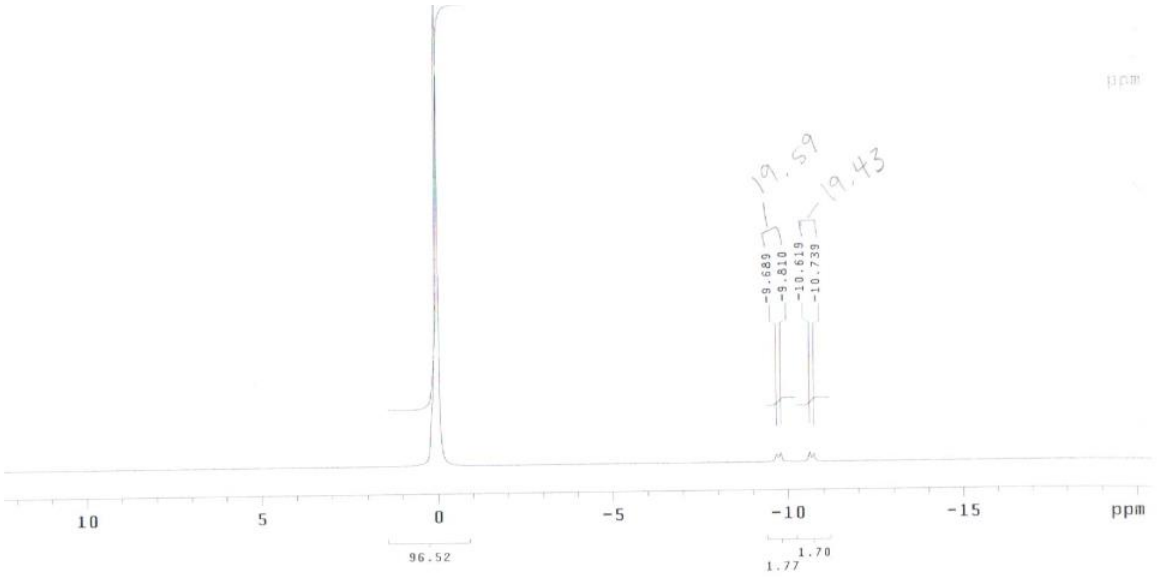

Figure 20. ^{31}P NMR of ADP at pH 4.4

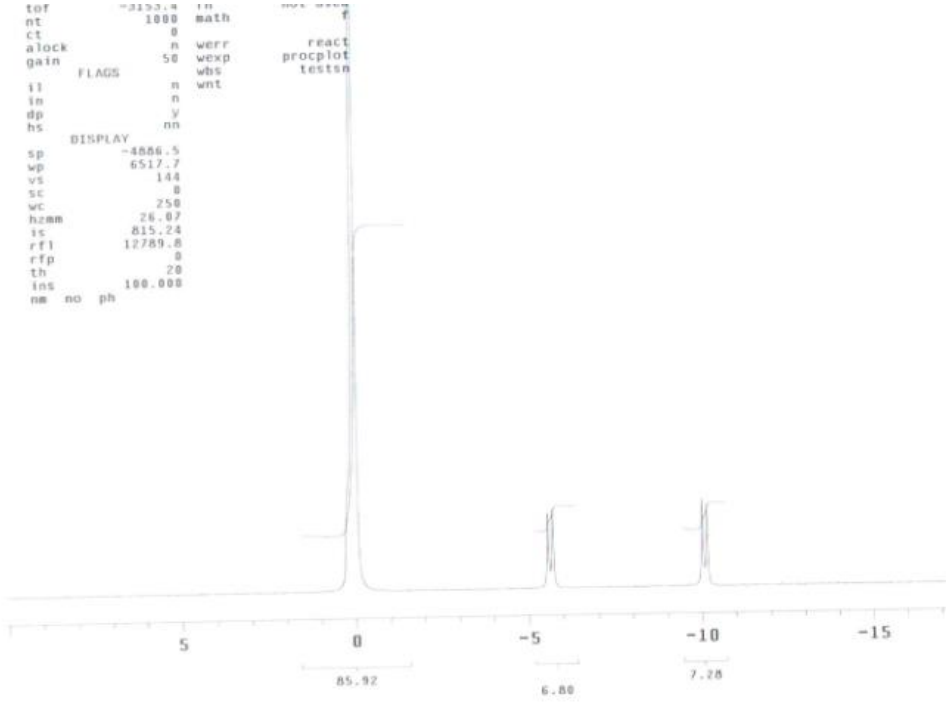

Figure 21. ^{31}P NMR of ADP at pH 8.5

Further efforts for characterization were attempted by subjecting the crude material from the reaction mixture and the phosphate positive column fractions to mass spectrometry. After we experienced problems obtaining reproducible data on the unknown fractions, known standard samples such as the SP_i starting material was also analyzed. After multiple samples and mass comparisons, mass spectrometry was determined to be an ineffective method for characterization. In the end, the obtained compound **A** did not display the characterization data to confirm the presence of the desired monothiopyrophosphate compound. While the conversion is described in literature, we observed no thiopyrophosphate generation through ^{31}P analysis of the reaction mixture. Future studies should be conducted in characterizing this compound because of its promising *in vitro* activity.

Since the obtained compound A proved to be inconsistent with monotriopyrophosphate, and the crude reaction mixture didn't show the presence of doublets, other synthetic method were explored to generate our desired compound. Another reported synthesis by Dunaway-Mariano[50] was used for

subsequent synthesis of the desired monothiopyrophosphate. Detailed in the experimental section, this particular procedure differed from the initial synthesis in regards to the drying and heating of the sample. The titrated white thiophosphate salt was subjected to six hours of drying under vacuum over P_2O_5 and two hours of heating at 153°C under vacuum. Increasing the drying time and reaction temperature could significantly decrease the amount of moisture present within the system, promoting the reaction to proceed. With the presence of any moisture, the reaction will not proceed forward to produce monothiopyrophosphate. If moisture is present within the reaction mixture, the reaction will show complete conversion of the starting material to pyrophosphate and other phosphate derivatives due to hydrolysis of higher order phosphate intermediates. Decreasing the heating time can also decrease the chance of phosphate polymerization, limiting the number of polyphosphate compounds generated during the reaction. The synthesis was conducted and a ^{31}P NMR was taken of the crude material in basic and acidic pH as seen in Figure 16 and Figure 17. The doublets at 37.41 ppm and -10.589 ppm (J=28.00 Hz) at pH 4.8 observed in these spectra suggest the presence of the SPP_i within the reaction mixture.

Purification of this crude material was attempted with HCl and K_2CO_3 elution systems. The Fiske and Subbarow assay was conducted on these fractions and the phosphate positive fractions were evaporated and analyzed with ^{31}P NMR. The NMRs of the HCl column fractions showed that the material was not recovered from the column, whether from decomposition or undetectable concentration levels. Returning to the literature procedure, a K_2CO_3 ion exchange column was conducted and analyzed with the Fiske and Subbarow assay. Precipitation was carried out with perchloric acid and proved to be difficult and inconsistent. While the initial precipitation afforded a high concentration of insoluble precipitate, the filtered fractions continued to generate solid precipitate throughout sample evaporation and processing. The overall procedure was tedious and required multiple filtration attempts and incubation in an ice bath. The fractions were concentrated and NMRs were taken of each sample. The 0.25 M fraction and the 0.3M fraction showed the presence of P_i and PP_i. The remaining fractions didn't

show the presence of any material. The loss of the compound is most likely due to either a low yielding reaction or loss of product during sample processing. A low yielding reaction can result in undetectable concentrations of product within the NMR sample. The multiple attempts of precipitate filteration and removal could have also contributed to the loss of product.

A TLC using polyetherimide (PEI)-cellulose plates with 1M NH_4HCO_3 was carried out on the reaction mixture along with a number of known standards such as P_i, SP_i, and PP_i. The TLC, as shown in Figure X was stained with an acetone (100.00 mL) based stain containing perchloric acid (3.00 mL), ammonium molybdate (1.00 g) and water (8.00 mL) which specifically detects the presence of phosphorous. Analysis of this plate shows that the reaction mixture is generating Pi, PPi, and three unknown products close to the baseline. Also, the reaction mixture showed no presence of the starting material, meaning complete consumption and conversation of the SP_i to products. Further characterization of these products along with development of the purification techniques is needed to verify the generation of monothiopyrophosphate.

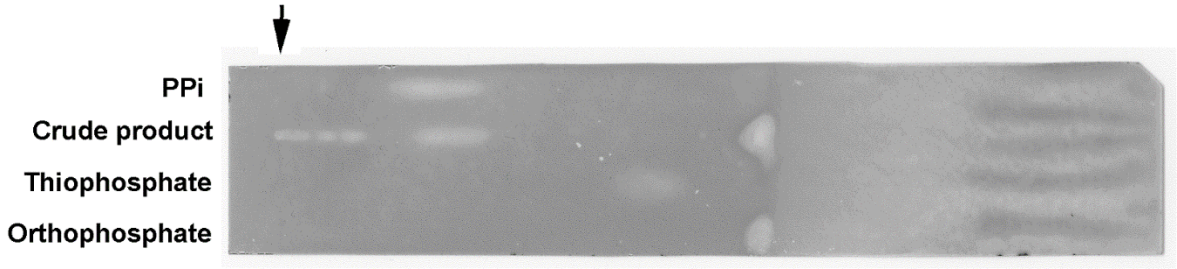

Figure 22. PEI-cellulose TLC of crude reaction product and related phosphate standards.

4. Conclusions and Future Studies

While the initial attempts for synthesis and characterization proved to be nonproductive, the alternative pyrolysis protocol afforded multiple phosphate derivatives within a crude mixture. The crude mixture was analyzed by ^{31}P NMR which showed strong evidence towards the generation of monothiopyrophosphate. Purification of this crude product is currently being developed along with TLC analysis. After purification, *in vitro* assays that examine hydroxyapatite formation and hydrolytic

activity by inorganic phosphatase and alkaline phosphatase should be performed to assess biological activity of this compound. If the *in vitro* assays show promising data, *in vivo* studies in wild-type and uremic rats should be explored to verify the efficacy of monothiopyrophosphate as a therapeutic inhibitor of vascular calcification.

Literature Cited

1. Valentine, JC, & McDonald, FE. (2006). Biomimetic synthesis of trans,syn,trans-fused polycyclic ethers. *Synlett*, *12*, 1816-1828.
2. Bartlett, PA, & Ting, PC. (1986). Construction of trans-fused polycyclic ethers:methodology for the brevetoxins. *Journal of Organic Chemistry*, *51*, 2230-2240.
3. Fleming, L. E., Kirkpatrick, B., Backer, L. C., Bean, J. A., et al. CHEST. 2007; 131(1):187-194
4. Baden, D. G., Bourdelais, A. J., Jacocks, H., Michelliza, S., Naar, J. Environ Health Perspect. 2005 May; 113(5): 621–625
5. (a) Nicolaou, K. C.; Reddy, K. R.; Skototas, G.; Sato, F.; Xiao, K.-Y. *J. Am. Chem. Soc.* **1992**, *114*, 7935. (b) Nicolaou, K. C.; Reddy, K. R.; Skokotas, G.; Sato, F.; Xiao, X.-Y.; Hwang, C.-K. *J. Am. Chem. Soc.* **1993**, *115*, 3558.
6. (a) Nicolaou, K. C.; Theodorakis, E. A.; Rutjes, F. P. J. T.; Tiebes, J.; Sato, M.; Untersteller, E.; Xiaou, X.-Y. *J. Am. Chem. Soc*. **1995**, *117*, 1171. (b) Nicolaou, K. C.; Rutjes, F. P. J. T.; Theodrakis, E. A.; Tiebes, J.; Sato, M.; Untersteller, E. *J. Am. Chem. Soc*. **1995**, *117*, 1173. (c) Nicolaou, K. C.; Hwang, C.-K.; Duggan, M. E.; Nugiel, D. A.; Abe, Y.; Bal Reddy, K.; DeFredds, S. A.; Reddy, D. R.; Awartani, R. A.; Conley, S. R.; Rutjes, F. P. J. T.; Theodrakis, E. A. *J. Am. Chem. Soc*. **1995**, *117*, 10227. (d) Nicolaou, K. C.; Theodrakis, E. A.; Rutjes, F. P. J. T.; Sato, M.; Tiebes, J.; Xiao, X.-Y.; Hwang, C.-K.; Duggan, M. E.; Yang, Z.; Couladouros, E. A.; Sato, F.; Shin, J.; He, H.-M.; Bleckman, T. *J. Am. Chem. Soc*. **1995**, *117*, 10239. (e) Nicolaou, K. C.; Rutjes,F. P. J. T.; Theodrakis, E. A.; Tiebes, J.; Sato, M.; Untersteller, E. *J. Am. Chem. Soc.* **1995**, *117*, 10252.
7. (a) Nicolaou, K. C.; Duggan, M. E.; Hwang, C.-K.; Somers, P. K. *J. Chem. Soc., Chem. Commun*. **1985**, 1359. (b) Nicolaou, K. C.; Prasad, C. V. C.; Somers, P. K.; Hwang, C.-K. *J. Am. Chem. Soc*.**1989**, *111*, 5330. (c) Nicolaou, K. C.; Prasad, C. V. C.; Somers, P. K.; Hwang, C.-K. *J. Am. Chem. Soc.* **1989**, *111*, 5335.
8. Lin, Y.-Y.; Risk, M.; Ray, S. M.; Van Engen, D.; Clardy, J.; Golik, J.; James, J. C.; Nakanishi, K. *J. Am. Chem. Soc*. **1981**, *103*, 6773. (b) Lee, M. S.; Repeta, D. J.; Nakanishi, K.; Zagorksi, M. G. *J. Am. Chem. Soc*. **1986**, *108*, 7855.
9. (a) Yasumoto, T.; Murata, M. *Chem. Rev.* **1993**, *93*, 1897. (b) Shimizu, Y. *Chem. Rev.* **1993**, *93*, 1685. (c) Murata, M.; Yasumoto, T. *Nat. Prod. Rep.* **2000**, *17*, 293. (d) Yasumoto, T. *Chem. Rec*. **2001**, *1*, 228, (e) Deranas, A, H.; Norte, M.; Ferna´ndez, J. J. *Toxicon* **2001**, *39*, 1101.
10. Matsuo, G.; Kawamura, K.; Hori, N.; Matsukura, H.; Nakata, T. *J. Am. Chem. Soc*. **2004**, *126*, 14374.
11. (a) Corey, E. J.; Ha, D.-C. *Tetrahedron Lett*. **1988**, *29*, 3171. (b) Matsuo, G.; Hori, N.; Matsukura, H.; Nakata, T. *Tetrahedron Lett*. **2000**, *41*, 7677.
12. (a) Hori, N.; Matsukura, H.; Matsuo, G.; Nakata, T. *Tetrahedron Lett*. **1999**, *40*, 2811. (b) Hori, N.; Matsukura, H.; Nakata, T. *Org. Lett*. **1999**, *1*, 1099. (c) Matsuo, G.; Hori, N.; Nakata, T. *Tetrahedron Lett*. **1999**, *40*, 8859. (d) Hori, N.; Matsukura, H.; Matsuo, G.; Nakata, T. *Tetrahedron* **2002**, *58*, 1853.
13. Molander, G. A.; Etter, J. B. *J. Am. Chem. Soc.* **1987**, *109*, 6556.
14. Peczuh, M. W.; Snyder, N. L.; Fyvie, W. S. *Carbohydrate Research*. **2004**, *339* 6 1163-1171
15. Peczuh, M. W.; Saha, J. *Advances in Carbohydrate Chemistry and Biochemistry*. **2011** *66*, 121-186
16. Micheel, F.; Sückfull, F. *Justus Liebigs Ann. Chem.***1933**, *502*, 85–98.
17. Micheel, F.; Spruck, W. *Ber. Dtsch. Chem. Ges. B*. **1934**, 1665–1667.
18. Pakulski, Z. *Pol. J. Chem.***2006**, *80*, 1293–1326.
19. Pakulski, Z. *Pol. J. Chem.* **1996**, *70*, 667–707.

20. Stevens, J. D. *Carbohydr. Res*. **2011**, *346*, 689–690. (b)Tran , T. Q; Stevens, J. D. *Aust. J. Chem*. **2002**, *55*, 171–178. (c) Driver, G. E.; Stevens, J. D. *Carbohydr. Res*. **2001**, *334*, 81–89. (d) Ng, C. J.; Craig, D. C.; Stevens, J. D. *Carbohydr. Res.* **1996**, *284*, 249–263. (e) Ng C. J.; Stevens, J. D. (1996) 241–248. (f) Driver, G. E.; Stevens, J. D. *Aust. J. Chem.* **1990**, *43*, 2063–2081. (g) Ng C. J.; Stevens, J. D. Methods Carbohydr. Chem. **1976**, *7*, 7–14. (h) Stevens, J. D. *Aust. J. Chem.* **1975**, *28*, 525–557.
21. Hoberg, J. O.; Bozell, J. J. *Tetrahedron Lett.* **1995**, *36*, 6831–6834.
22. Castro, S.; Peczuh, M. W. *J. Org. Chem.* **2005**, *70*, 3312–3315.
23. E. Alcazar, J. M. Pletcher, and F. E. McDonald. *Org. Lett.* **2004**, *6*, 3877–3880.
24. McDonald, F. E. *Chem. Eur. J.* **1999**, *5*, 3103–3106.
25. Koo, B.; McDonald F. E. *Org. Lett.* **2007**, *9*, 1737–1740.
26. Boone, M. A.; McDonald, F. E.; Lichter, J.; Lutz, S.; Cao, R.; Hardcastle, K. I.; *Org. Lett.* **2008**, *11*, 851-854
27. Hughes, N. A.; Speakman, P. R. H. *Carbohydrate Res.*, **1965** *1* 171-175
28. Pietruszka, J.; Witt, A.; *Synthesis* **2006** *24* 4266-4268
29. Russo D, Palmiero G, De Blasio AP, Balletta MM, Andreucci VE. *Am J Kidney Dis*. 2004;44:1024-1030.
30. Campean V, Neureiter D, Nonnast-Daniel B, Garlichs C, Gross ML, Amann K *Atherosclerosis*. 2007;190:156-166.
31. Nakamura S, Ishibashi-Ueda H, Niizuma S, Yoshihara F, Horio T, Kawano Y. *Clin J Am Soc Nephrol*. 2009;4:1892-1890.
32. Mehrotra R, Adler S. *Am J Kidney Dis*. **2005** *45* 963.
33. Raggi P, Boulay A, Chasan-Taber S, Amin N, Dillon M, Burke SK, Chertow GM. *J Am Coll Cardiol*. **2002** *39* 695-701.
34. London GM, Guerin AP, Marchais SJ, Metivier F, Pannier B, Adda H. *Nephrol Dial Transplant*. **2003** *18* 1731-1740.
35. O'Neill, WC; *Kidney International*, **2007** *71* 282-283
36. Persy, VP; McKee, MD; *Kidney International* **2011** *79*, 490 – 493
37. O'Neill, WC*;* Lamashvili, KA; *Kidney International* **2010** *78***,** 1232–1239
38. Jung A, Bisaz S, Fleisch H. *Calcif Tiss Res*. **1973** *11* 269-280.
39. Fleisch H, Russell RGG, Bisaz S, Muhlbauer RC. *Europ J Clin Invest*. **1970** *1* 12-18.
40. Turhanen P, Demadis KD, Peraniemi S, Vepsalainen JJ. *J Org Chem*. **2007** *72* 1468-1471.
41. Yatzidis H. *Clin Nephrol*. **1985** *23* 63-67.
42. Yatzidis H, Agroyannis B. *Perit Dial Bull*. **1987** *7* 250-252.
43. Cicone JS, Petronis JB, Embert CD, Spector DA. *Am J Kidney Dis*. **2004** *43* 1104-1108.
44. Price PA, Roublick AM, Williamson MK. *Kidney Int*. **2006** *70* 1577-1583.
45. Price PA, Faus SA, Williamson MK. *Arterioscler Thromb Vasc Biol*. **2001** *21* 817-824.
46. Tamura K, Suzuki Y, Matsushita M, Fujii H, Miyaura C, Aizawa S, Kogo H.. *Eur J Pharmacol*. **2007** *558* 159-166.
47. O'Neill WC, Lomashvili KA, Malluche HH, Faugere M-C, Riser BL. *Kidney Int*. **2011** In press.
48. Cheung HS, Sallis JD, Demadis KD, Wierzbicki A. Phosphocitrate blocks calcification-induced articular joint degeneration in a guinea pig model. *Arthritis Rheum*. **2006** *54* 2452-2461.
49. Lin, I.; Knight, Wilson B.; Hseuh, A; Dunaway-Mariano, D. *Biochemistry* **1986** *25* 4688-4692
50. Dunaway-Mariano, D. *Tetrahedron* **1976** *32* 2991 – 2996
51. Fiske, CH; Subbarow, Y. *The Journal for Biological Chemistry*. *77* 375-400